Editorial Manager(tm) for Bulletin of the Seismological Society of America
Manuscript Draft

Manuscript Number: BSSA-D-08-00209R1

Title: Inter-event and inter-station variability computed for the Italian Accelerometric Archive (ITACA) (previous title: Inter-event and inter-station variability from new Italian ground motion prediction equations)

Article Type: Article

Section/Category: Regular Issue

Corresponding Author: Dino Bindi,

Corresponding Author's Institution: Istituto Nazioanale di Geofisica e Vulcanologia

First Author: Dino Bindi, PhD

Order of Authors: Dino Bindi, PhD; Lucia Luzi; Francesca Pacor

Abstract: The inter-event and inter-station ground motion variability of the updated Italian strong-motion database (ITACA) has been explored through the development of new empirical Ground Motion Prediction Equations (GMPEs) for Italy. The regressions have been performed on 241 three-component waveforms from 27 earthquakes with moment magnitude ranging from 4.8 to 6.9, recorded by 146 stations at distances up to 200 km. The site classification follows the schemes previously proposed for Italy, in which two soil classes are defined, considering both shear wave velocity and deposit thickness. The regression analyses uses the values of the explanatory variables (magnitude, fault distance, site class, and style of faulting) recently revised in the framework of a project funded by the Italian Department of Civil Protection. The equations have been derived for peak ground acceleration, peak ground velocity and 5% damped spectral accelerations at 18 periods from 0.03 to 2 seconds.
The residual variance has been decomposed into inter-event, inter-station and record-to-record components by applying a random effect regression scheme. The inter-event and inter-station error distributions have been analyzed as function of periods, to detect sites and events for which predicted values significantly deviate from observations. For periods up to 0.35s, the inter-station is the dominant component of variance, indicating that an improvement in the site classification could lead to a refinement of the GMPEs. For longer periods, the three components of variance provide similar contributions, indicating that a reduction of the uncertainty can be achieved by reducing the epistemic uncertainty affecting the physical model. The inter-event error highlights the peculiarity of few earthquakes, suggesting that the evaluation of regional GMPEs can be important when specific scenario studies should be carried out. The inter-station variability allows to detect stations with peculiar site response and to assess the goodness of the considered site classification scheme.

Suggested Reviewers:

Opposed Reviewers:

Response to Reviewers: I will upload the letter to AE in a later step

Milano,

26 February 2009

Manuscript number BSSA08-00292

Title *'Inter-event and inter-station variability computed for the Italian Accelerometric Archive (ITACA)'*

(previous title *Inter-event and inter-station variability from new Italian ground motion prediction equations*)

Authors: *Bindi, Luzi, Pacor*

Dear Gail Atkinson,

Enclosed please find the revised version of our manuscript number BSSA-00292.

The main suggestions/criticisms raised by the reviewer and by the AE are about the arguments supporting the need of developing new GMPE using the data considered in the manuscript and to show comparisons with NGA results. In particular, the motivations for developing new GMPEs do not appear to be strong enough and the comparison with the NGA models could be carried out within the debate about the performance of global versus regional models.

These constructive criticisms allowed us to understand that the main target of our manuscript was not well exposed. In particular, we probably emphasized too much the development of new GMPE for Italy while the main aim of our work was the analysis of residuals through the estimation of the inter-event, inter-station and record-to-record components of variance. The improvements about the recordings metadata provided by the new Italian strong-motion data set (http://itaca.mi.ingv.it ;Luzi et al., 2008) allowed us to derive new models for Italy that we used as reference for our residual analysis, which are the main contribution of our work, as also observed and favourably commented by the reviewer. The analysis we performed represents a tool that will be largely applied to check the quality of ITACA recordings and metadata in the framework of some Italian ongoing projects.

Then, the revised manuscript has been re-organized in order to focus the attention of the reader mainly on the analysis of variability we performed. Since the models we developed for analyzing the residuals represent an update of the Italian one (Sabetta and Pugliese 1996), their reliability is still discussed in the revised manuscript but this part has been shortened and moved at the end of the manuscript.

Another point raised by the reviewer was the comparison with Stewart et al. (2008). With respect to the purposes of our manuscript, the main interesting comparison with Stewart et al. (2008) could be

the site classification. This classification was based also on some shear-wave profiles (obtained from SASW measurements) performed at some Italian sites. In the framework of a new Italian project (http://esse4.mi.ingv.it, 2007-2009), further geophysical investigations have been promoted for increasing the number of stations characterized by shear-wave profiles and alternative scheme of classification will be tested. Since these tasks are still ongoing, we prefer to present the results only when all the planned activities will be carried out. The analysis of the new findings will allow us to perform a more detailed comparison with Stewart et al. (2008).

The comparison between global and regional models is of great interest and faced by several authors. As an example, Strafford et al (2007) showed the applicability of the NGA models to Europe, confirming the findings of Campbell and Bozorgnia (2006). We believe that any further thorough comparison is beyond the aim of the present manuscript and, furthermore, it would require regional data set larger than the one we analyzed here. The improvement introduced by the ITACA database only allows to update the GMPE models for Italy, as the Italian data represent a small subset of a region, such as the Mediterranean area. We are planning to share our data with other Mediterranean countries in order to develop robust models comparable to NGA. For example, in Figure R1 we show the magnitude versus distance distribution of Italian data we are preparing. These data will be added to data sets coming from Turkey, Greece and Balkans put together by colleagues from these countries. After that, we will probably have a data set suitable for reliable discussions about the differences between the Mediterranean models and those derived for other regions (e.g. Japan, Taiwan, Eastern USA) or differences with predictions from global models like NGA.

Since no technical issues were raised by the reviewer, the analysis in the manuscript have been not changed but the overall exposition rearranged. In order to organize our manuscript according to your suggestions and to better clarify the true aim of this work, we modified the title, we rewrote the introduction and abstract and we re-organized the text. We performed all the minor changes pointed out by the reviewer and the Associate Editor, such as the change of the symbols used to identify the error distributions, the suggested references were added, and a couple of figures removed. We better clarified that, in order to make possible the comparison with the Molise and Umbria-Marche regional models (Figure 14 of the revised manuscript), a further regression for PGA was also performed considering the hypocentral distance. About the non-linear site effects, we have not included a term accounting for such a behaviour because, as already pointed out by Akkar and Bommer (2007), even enlarging to the European data set, the recordings do not allow to constrain this term in the attenuation model.

Finally, we would like to acknowledge both the reviewer and you for all the suggestions which helped us to better focus our analysis. Looking forward to receive your further communications about our manuscript,

Sincerely
Dino Bindi

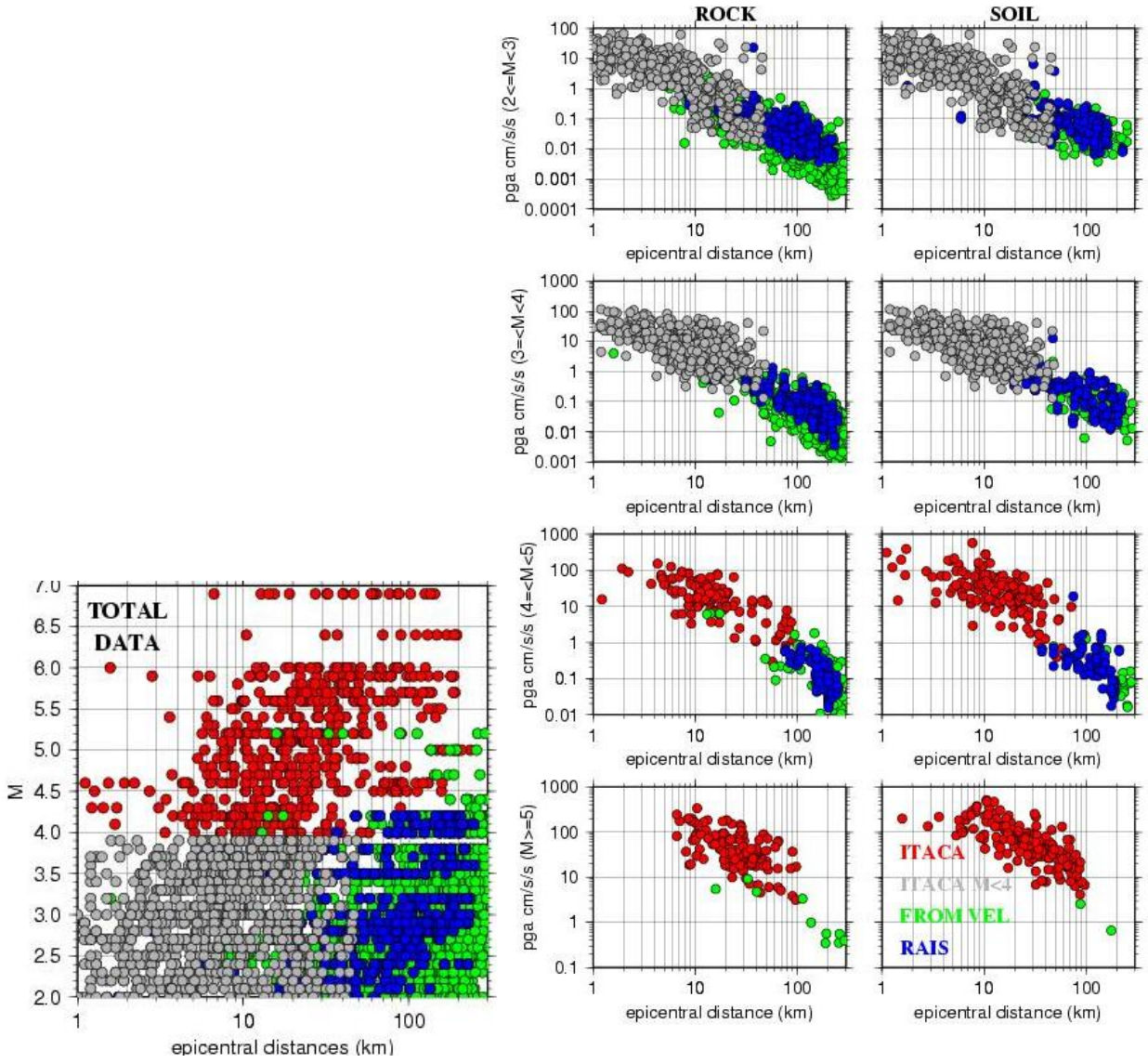

Figure R1. Magnitude versus distance scatter plot (left) and PGA versus distance (right) (preliminary analysis). The different colours indicate different Italian data set. The ITACA data used in the manuscript are in red, while the grey circles are data in ITACA but not used in the manuscript because of the assumed magnitude cut-off; the blue circles are data from a strong motion network installed in north Italy; the green circles are data from seismometers installed in north Italy.

Version**: 26 February 2009**

Inter-event and inter-station variability computed for the Italian Accelerometric Archive (ITACA)

D. Bindi[(1)], L. Luzi[(1)], F. Pacor[(1)]

[(1)] Istituto Nazionale di Geofisica e Vulcanologia, Via Bassini 15, 20133 Milano, Italy

Corresponding Author: Dino Bindi, bindi@mi.ingv.it, tel +39 0223699270, fax +39 0223699458

Abstract

The inter-event and inter-station ground motion variability of the updated Italian strong-motion database (ITACA) has been explored through the development of new empirical Ground Motion Prediction Equations (GMPEs) for Italy. The regressions have been performed on 241 three-component waveforms from 27 earthquakes with moment magnitude ranging from 4.8 to 6.9, recorded by 146 stations at distances up to 200 km. The site classification follows the schemes previously proposed for Italy, in which two soil classes are defined, considering both shear wave velocity and deposit thickness. The regression analyses uses the values of the explanatory variables (magnitude, fault distance, site class, and style of faulting) recently revised in the framework of a project funded by the Italian Department of Civil Protection. The equations have been derived for peak ground acceleration, peak ground velocity and 5% damped spectral accelerations at 18 periods from 0.03 to 2 seconds.

The residual variance has been decomposed into inter-event, inter-station and record-to-record components by applying a random effect regression scheme. The inter-event and inter-station error distributions have been analyzed as function of periods, to detect sites and events for which predicted values significantly deviate from observations. For periods up to 0.35s, the inter-station is the dominant component of variance, indicating that an improvement in the site classification could lead to a refinement of the GMPEs. For longer periods, the three components of variance provide similar contributions, indicating that a reduction of the uncertainty can be achieved by reducing the epistemic uncertainty affecting the physical model. The inter-event error highlights the peculiarity of few earthquakes, suggesting that the evaluation of regional GMPEs can be important when specific scenario studies should be carried out. The inter-station variability allows to detect stations with peculiar site response and to assess the goodness of the considered site classification scheme.

Introduction

In Italy, strong-motion recordings are available since the early seventies. Since different institutions managed the Italian strong motion network (RAN, Rete accelerometrica italiana), both waveforms and metadata needed to qualify the recordings are hardly available to end-users, except for few cases, such as the 1997-98 Umbria-Marche sequence and the 2002 Molise earthquakes (see Data and Resources Section). The Italian *Dipartimento di Protezione Civile* (DPC, Italian Department for Civil Protection) after an agreement with *Istituto Nazionale di Geofisica e Vulcanologia* (INGV, Italian Institute for Geophysics and Volcanology) funded in 2004 the project *Database dei dati accelerometrici italiani relativi al periodo 1972-2004* (Italian strong-motion database relevant to the period 1972-2004, hereinafter referred to as project *S6*, see Data and Resource Section). The aim of the project was the revision of the entire strong motion data-set acquired over the period 1972-2004 in Italy by different institutions, namely Ente Nazionale per l'Energia Elettrica (ENEL, *Italian electricity company*), Ente per le Nuove tecnologie, l'Energia e l'Ambiente (ENEA, *Italian energy and environment organization*) and DPC. The seismic event, station and instrument metadata have been revised and the raw recordings have been individually processed in order to obtain reliable estimates of acceleration, velocity and acceleration response spectra. The main result of the project is represented by the online Italian Accelerometric Archive (ITACA) (Luzi et al., 2008) where strong-motion recordings of earthquakes occurred in Italy can be downloaded and the metadata about stations and earthquakes can be accessed (see Data and Resources Section).

An important step in the seismic-hazard assessment is the development of empirical ground-motion prediction equations (GMPEs). These equations are typically determined by fitting the assumed ground motion model to a set of observed strong-motion parameters, such as the logarithm of the peak ground acceleration, velocity, displacement or different spectral ordinates at several periods. After the parameters of the model have been determined through the regression analyses, the GMPE allows the prediction of the ground-shaking level once the predictor variables are assigned. Besides the predicted median values, the random variability of ground motions plays an important role in the seismic-hazard assessment (e.g. Chen and Tsai, 2002;Atkinson, 2006; Morikawa et al., 2008) . A recent review about the current state of knowledge regarding the estimation of the random variability can be found in Strasser et al. (2009).

In this paper, we aim at evaluating such variability by considering the recordings collected in the ITACA database. To accomplish this task, we develop a new set of GMPEs considering 27 earthquakes belonging to ITACA with moment magnitude in the range 4.8-6.9. These earthquakes were recorded at distances up to 200 km by 146 stations for which geological and geophysical data are available. Since the ground motion variability is generally described in terms of standard

deviation of residuals about the mean predictions, we apply the random effect model (e.g. Abrahamson and Youngs, 1992) to identify the different components of variance for the ground-motion random variability. In particular, we isolate and discuss both the inter-event and inter-station distribution of errors in order to identify those earthquakes and recording stations with peculiar behaviour, worthy of further investigations.

Data set

The project *S6* provided a revised strong motion database of the earthquakes occurred in Italy from 1972 and 2004, recorded by the ENEL, RAN and ENEA networks (Luzi at al., 2008). Hypocentral parameters, magnitudes and station locations have been verified and updated and the geological, geophysical and geotechnical information about the recording sites have been collected and included, as well as the results from new geotechnical surveys promoted within the project.

For this study a subset of 27 events (Table 1 and Figure 1) was extracted from the ITACA database (Data and Resources Section), with moment magnitude ranging from 4.6 (Irpinia aftershock, 1980) to 6.9 (Irpinia, 1980). Most of the events were caused by normal faults in central and southern Apennines and few of them had either strike-slip (Ancona, 1972; Potenza, 1990; Eastern Sicily, 1990; Molise, 2002) or reverse-slip (1976 Friuli sequence; Southern Tyrrhenian, 2002) mechanisms. Table 1 lists the main features of the 27 earthquakes. The hypocentral parameters of the selected events were obtained by the ING Catalogue for the events in the period 1972 – 1982 and by the Catalogue of Italian Seismicity (CSI) for the events subsequent to 1982 (Data and Resource Section). Complex events, localised offshore or showing large horizontal errors in the catalogue, were relocated using other procedures (Mele et al., 2002). The moment magnitude was obtained by global or regional catalogues. In general the moment magnitude for events with $M > 5.0$ was determined by the Global Centroid Moment Tensor Project, while for weaker events the Regional Centroid Moment Tensor (Pondrelli et al., 2006) and Earthquake Mechanisms of the Mediterranean Area (Vannucci and Gasperini, 2004) were used.

Within the project *S6*, a careful revision of the characteristics of the recording sites was also performed, from their relocation using the same geographic map projection referred to the international ellipsoid WGS84. An extensive collection of geological, geophysical and geotechnical studies of the past 30 years was performed and about 20 shear wave velocity profiles derived by cross-hole and down-hole tests performed by different institutions and private companies were obtained. They were useful to characterise the accelerometric sites that recorded the major Italian earthquakes. The rest of the sites has been qualified through an integrate analysis of geologic information and earthquake records. In particular, it was possible to perform HVSR on strong and

weak motions and, in few cases, SSR where the site was close to a reference station located on rock outcrop. In addition, several literature studies were used to infer information on site response of the accelerometric stations (Sanò et al., 1998; Rovelli et al., 2001; Rovelli et al., 2002; Cultrera et al., 2003; Castro et al., 2004; Luzi et al., 2005).

In this study, we use all the available information to classify the sites as proposed by Sabetta and Pugliese, (1987), hereinafter referred to as SP87, and Sabetta and Pugliese, (1996), hereinafter referred to as SP96. The authors recognized 3 classes according to geological and geotechnical information and thickness of the soil layer: 1) "rock" (class 0, rock outcrops or deposits with thickness lower than 5m); 2) "shallow alluvium" (class 1, deposits with thickness lower than or equal to 20m) and 3) "deep alluvium" (class 2 deposits with thickness greater than 20m), where alluvium refers to deposits with shear wave velocity between 400 m/s and 800 m/s. The validation process based on the information collected by the S6 project led to the re-classification of 14 sites with respect to SP87 (Table 2). In particular, 7 stations were moved from class 0 to class 1 and 4 sites, previously included in class 2, have been re-classified as class 1. Most of the differences (5 cases) concerned the stations which recoded the M_w = 6.9, 1980 Irpinia earthquake, the strongest event of the dataset.

In total, we considered 241 three-components recordings from 146 stations (98, 62 and 81 for class 0, 1, and 2, respectively) with magnitude range from 4.6 to 6.9 and fault distances range from 0 to 190 km (Figure 2). The Joyner-Boore distance has been computed for the events with M >= 5.5 using the fault geometry reported in the DISS database (Basili et al., 2008; see Data and Resources section) whereas the epicentral distance has been considered for the other earthquakes. The near-source distances are poorly represented by the data-set: 11 recordings from three earthquakes (EveId's 14, 21 and 22 in Table 1) have distances smaller than 5 km whereas earthquakes of magnitude 6.4 and 6.9 were recorded only at distances larger than 7 km. The focal depths vary from 2 to 29 km and the best sampled intervals are 10-100 km for distance and 5–6 for magnitude. The majority of the events have been recorded by at least 4 stations, with a maximum of 25 records for the third strongest shock (Mw 5.6) of the Umbria-Marche sequence (eveID=23 in Table 1).

Data processing

The data set includes a large number of accelerograms recorded by analogue instruments, mainly Kinemetrics SMA-1, which were widespread on the Italian territory before the 90's, together with records obtained by digital instruments. Two different data processing procedures were adopted. The analogue records were corrected for the linear trend and for the instrument response. Then the time-series were band-pass filtered, selecting the high pass frequency from the visual inspection of

the Fourier spectrum. In average, the high pass frequency was selected in the range between 0.3-0.5 Hz. The low-pass frequency was selected close to the instrument frequency, generally centred between 20-25 Hz. For the digital records the linear trend fitting the entire record was removed, instead of the common practice of using the pre-event trace, as very few records had a useful pre-event. A band pass filter was applied selecting the high pass frequency similarly to the analogue records, but shifted toward lower values (0.1-0.3 Hz) while the low-pass frequency was generally applied in the range 25-30 Hz. A raised cosine filter was used for the analogue records, which are often triggered on the S-phase, while an acausal 4^{th} order Butterworth was used for the digital signals, which were opportunely padded with zeros in order to mitigate the filter transient effects at both beginning and end of the record.

The Irpinia earthquake is composed by three separate events; the first one occurred on 1980-11-23 at 18:34:53 GMT and was followed by other two shocks with a delay of about 20 and 40 seconds (Boschi et al., 1993). In the near–source recordings the three events are well recognizable. In this case we used magnitude and focal parameters relevant to the first shock, and, as consequence, we considered only the first event for the selection of the peak values. The earthquakes with eveID=2, 5, 7, 12, 13, 15, 17 (Table 1) are also part of the flat file prepared by the Pacific Earthquake Engineering Research Center's (PEER) for the Next Generation Attenuation (NGA) project (Power et al., 2006), while the earthquakes included in the European database have the eveID shown in bold.

Functional forms

The information available in the ITACA database allows us to develop a GMPE considering a more complex functional form than the one generally adopted for Italian territory (Sabetta and Pugliese, 1987; 1996). In this study, the GMPEs are derived considering the functional form used by Akkar and Bommer (2007) for the new European peak ground velocity equations. The model includes both a quadratic term in magnitude and magnitude-dependent attenuation term. As predictor variables, we consider the moment magnitude (Mw), the Joyner-Boore distance (R_{JB}), the site class and the style-of-faulting. The equations are derived for peak ground acceleration (PGA), peak ground velocity (PGV), and 5%-damped spectral acceleration (SA) at 18 periods from 0.03 to 2s, considering both the larger (hereinafter indicated with the prefix *max*) and the geometric mean (hereinafter *geo*) of the horizontal components, as well as the vertical component (hereinafter *vert*). The functional form is the following:

$$\log_{10} Y = a + b_1 (M_W - M_{ref}) + b_2 (M_W - M_{ref})^2 + (c_1 + c_2 (M_W - M_{ref})) \log_{10} \sqrt{(R_{JB}^2 + h^2)} + e_i S_i + f_j F_j \quad (1)$$

where Y is the response variable; M_{ref} is a reference magnitude; S_i with i=1,2,3 are dummy variables that assume either the value 0 or 1 depending on soil type (rock: S_1=1 and S_2=S_3=0; shallow alluvium: S_2=1 and S_1=S_3=0; deep alluvium: S_3=1 and S_1=S_2=0); F_j are dummy variables that take either the value 0 or 1 depending on the style of faulting (normal fault: F_1=1 and F_2=F_3=0; strike-slip: F_2=1 and F_1=F_3=0; reverse fault: F_3=1 and F_1=F_2=0); e_i and f_j are the site and the style-of-faulting coefficients, respectively. In order to reduce the trade-off between attenuation and source contributions to the ground motion, the reference magnitude M_{ref} in equation (1) is set to 5.5. Following Brillinger and Preisler (1985) and Abrahmson and Youngs (1992), a random effect model is introduced to describe the error terms as follows:

$$\log_{10} Y_{ij} = \Gamma(M_i, R_{ij}, S_j, F_i; \mathbf{x}) + \eta_i + \varepsilon_{ij} \quad (2)$$

where Y_{ij} is the ground motion parameter for the earthquake *i* recorded by station *j*, $\Gamma(M_i,R_{ij},S_j,F_i;\mathbf{x})$ is the predictive equation with the explanatory variable M (magnitude), R (distance), S (site class) and F (style of faulting class), and $\mathbf{x}$=[a, b_1, b_2, c_1, c_2, h, $e_{1,2,3}$, $f_{1,2,3}$] is the vector of model coefficients. In equation (2), η_i represents the inter-event variations and ε_{ij} represents the intra-event variations. η_i and ε_{ij} are assumed to be independent, normally distributed with variances σ^2_{event} (inter-event component of variance) and $\sigma^2_{intra\text{-}event}$ (intra-event component of variance), respectively. In particular, σ^2_{event} measures the variability of the residuals for different stations that recorded the same event. The variance of $\log_{10}$Y in equation (1) is given by:

$$\sigma^2 = \sigma^2_{event} + \sigma^2_{intra\text{-}event} \quad (3)$$

The variability among sites can also accounted for (e.g. Chen and Tsai, 2002; Bindi et al., 2006; Bindi et al. 2007). In this case, the random effect model takes the following form:

$$\log_{10} Y_{ij} = \Gamma(M_i, R_{ij}, S_j, F_i; \mathbf{x}) + \varphi_j + \gamma_{ij} \quad (4)$$

where φ_j and γ_{ij} represent the inter-station and intra-station distribution of errors, respectively, assumed to be independent normally distributed with variances $\sigma^2_{station}$ and $\sigma^2_{intra\text{-}station}$. In particular, $\sigma^2_{station}$ measures the variability of the residuals for different earthquakes recorded by the same station. In the case of model (4), the variance of $\log_{10}$Y is given by the sum

$$\sigma^2 = \sigma^2_{station} + \sigma^2_{intra\text{-}station} \quad (5)$$

We also evaluate the record-to-record component of variance, that can be associated to both source (e.g. directivity) and propagation effects, given by:

$$\sigma^2_{record} = \sigma^2 - \sigma^2_{station} - \sigma^2_{event} . \quad (6)$$

Empirical Ground Motion Prediction Equations

The regression coefficients obtained for the GMPEs calibrated in this study for equation (1) are listed in Tables 3 – 5 for horizontal (*max and geo*) and vertical component.

The mean value and the standard error of each coefficient have been estimated by applying the bootstrap technique (e.g., Efron and Tibshirani, 1994). The bootstrap method consists in repeated inversions (500 times in our case) considering several datasets, called bootstrap samples, obtained by randomly sampling, with replacement, the set of observations. Each bootstrap sample has the same size of the original dataset (and all the constraints are preserved in each sample) and the bootstrap estimates of the standard errors are given by the standard deviations of the parameter distributions (called bootstrap replications) obtained for each bootstrap sample. The mean values are very similar to those obtained considering the original dataset without applying any re-sampling and the standard errors are mainly controlled by the trade-off among parameters not completely removed by the applied constraints. At certain periods, the regression coefficients showing standard deviation much larger than the mean value are not significantly different from zero (Tables 3, 4 and 5). For example, the coefficient b_2 relevant to the squared magnitude term is significant only for periods T larger than 0.35 s. Also the magnitude-dependent geometrical spreading coefficient c_2 and the style of faulting parameters are generally not significantly different from zero. The result about c_2 suggests that the magnitude-distance distribution shown in Figure 2 does not allow to capture the differences in the attenuation between moderate and small earthquakes. The small number of reverse and strike slip earthquakes included in the data set does not allow to capture systematic differences among the ground motions generated by different tectonic regimes. Nevertheless, following the discussions in Ambraseys et al. (2005a, pages 16-17), we keep all the coefficients for computing the predicted values.

The coefficient c_1 increases with increasing period, from -1.3 at 0.03 s to -0.94 at 2 s. This behaviour agrees with a decrease of the contribution of the anelastic attenuation with decreasing frequency. The site corrections for both class 1 and 2 are significantly different from zero. The site coefficients e_2 of equation (1), accounting for the amplifications of shallow alluvium, assumes the largest value for short periods and decreases for long periods. The largest values (up to 0.3122) are obtained for periods between 0.15 and 0.40 s. On the contrary, the site coefficients e_3, which

accounts for amplifications of deep sediments, assumes the largest values for periods longer than 0.6 s, reaching the maximum value of 0.3953 at 1 s.

Figure 3 exemplifies the main results for maximum, geometric mean between horizontal components and vertical component, showing the predicted PGA and PGV decay with Joyner-Boore distance for two different moment magnitudes (6.9 and 4.6). For M_w=6.9, maxPGA and geoPGA are similar, whereas geoPGV is slightly lower than maxPGV, but the difference diminishes with distance. Beyond 100 km the two trends match. About the vertical component, vertPGA is close to maxPGA at short distances but shows a more rapid decay with distance. The ratio between maxPGV and vertPGV is about 1.75 at 10 km and increases to 1.95 at 100 km.

For Mw=4.6, both geoPGA and geoPGV are slightly smaller than maxPGA and maxPGV, whereas the ratios maxPGA over vertPGA and maxPGV over vertPGV slightly increase with distance. The maximum horizontal over vertical ratio at 10 km is 2.6 and 3 for PGA and PGV, respectively; at 100 km these ratios increase to about 3.

Tables 6, 7 and 8 list the standard deviations obtained for the spectral accelerations at each period, as well as the results for PGA and PGV. The total standard deviation varies between 0.2963 and 0.3493 for maxH, between 0.2975 and 0.3404 for the geoH, and from 0.2686 to 0.3469 for the vertical component. These values are of the same order of magnitude of the GMPEs derived for many regions worldwide (Strasser et al., 2009).

To check whether the estimated mean values match the observations, the bias and its dependence on the predictor variables have been computed adopting the maximum-likelihood approach described in Spudich et al. (1999). The results for maxPGA shown in Figure 4 (panel a), are representative of the other response variables. The bias is nearly zero (0.0045 ± 0.0595), and its dependence on magnitude and logarithm of distance is negligible (panels (c) and (d) of Figure 4).

Since the zero bias and the absence of the residual dependence on the two explanatory variables confirm the suitability of the developed GMPE to describe the median behaviour of the observed ground motion, in the following we analyze the distribution of errors computed with respect to this model.

Inter-event distribution of error

The analysis of the inter-event distribution allows to quantify the error associated to each event of the dataset, when the ground motion is predicted with model (1).The inter-event error η_i, defined in equation (2), is shown for each earthquake in Figure 5, considering the maxPGA. The earthquakes are sorted by the earthquake identification number (eveID) given in Table 1. All the earthquakes show errors within the ±0.2 range, with the exception of the second main-shock of the Molise 2002

sequence (eveID=27) and the 1990 Eastern Sicily earthquake (eveID=20), that are overestimated and underestimated by the predictions, respectively.

Figure 6 shows the inter-event errors as function of period for all strike-slip (top panel) and reverse-slip (middle panel) earthquakes, and for a selection of normal-faulting earthquakes (bottom panel). The smallest dispersion is observed for normal earthquakes while the largest variability affects the strike-slip events with the two Molise earthquakes showing negative errors over the entire range of periods. Since both the parameters f_2 (strike-slip) and f_3 (reverse-slip) are generally very small (Tables 3 - 5), they slightly affects the predicted values. The inter-event error is positive for the mainshock of the Friuli sequence, which is the only moderate (Mw=6.4) reverse-slip earthquake included in the data set.

The under-estimation of the 1990 eastern Sicily could be partially attributed to the uncertainties affecting the location and magnitude of this off-shore earthquake. For example, the moment magnitude used for this earthquake is 5.6 but others works (e.g. Laurenzano and Priolo, 2005) considered a magnitude of 5.8. Also the over-estimation of the 2002 South Tyrrhenian off-shore earthquake (eveID=25) could be related to the uncertainties affecting its locations and magnitude or to significant difference in the attenuation properties. The propagation efficiency of the Adria micro-plate (Castro et al., 1999) could be the reason for the under-estimation of the peak values for the 1972 Ancona earthquake (eveID=1). The lower than expected level of shaking observed after the Molise earthquake has been ascribed to either a deficiency in the energy emitted by the source (A. Rovelli, personal communication) or to a propagation effect related to the strong velocity inversion at depth just above the area where the two mainshocks originated (Malagnini and Mayeda, 2008).

The estimated inter-event errors are used to correct the residuals shown in the panel (a) of Figure 4. After this correction (Figure 4, panel b), the residual dispersion is significantly reduced for the recordings of few earthquakes (the 1990 Eastern Sicily earthquake and the two 2002 Molise earthquakes) but it is still significant, indicating that the uncertainties on the event parameters are not the main source of the ground motion variability for this data-set.

Inter-station distribution of error

The analysis of the inter-station distribution allows to quantify the error associated to each station of the dataset, when the ground motion is predicted by equation (1). The inter-station error φ_j, defined in equation (4), is shown for each station in Figure 7, considering the maxPGA.

Most of the errors have absolute values smaller than 0.3 and only few stations show absolute errors larger that 0.4. In particular, the largest under-estimation is observed for the Catania Piana station

(CAT), for which the high peak ground accelerations recorded after the 1990 Eastern-Sicily earthquake have been previously recognized by Di Bona et al. (1995). The empirical site response estimated by computing the horizontal-to-vertical spectral ratio of both earthquake and microtremor recordings (Laurenzano and Priolo, 2005) detects the fundamental mode of vibration at 1.5 Hz, corresponding to the resonance frequency of a thin alluvial deposit (about 30 m) with average shear wave velocity of 195 m/s. The empirical site amplifications estimated from the 1990 earthquake records show a second peak between 4-6 Hz but the origin of this peak is unknown.

On the other hand, the largest PGA over-estimations are relevant to two rock stations (class 0) that recorded the Molise earthquakes (*Castiglione Messer Marino, CMM,* and *S. Marco dei Cavoti, SCV*) and to one deep alluvium site (class 2) *L'Aquila-Valle Aterno-Aquilpark* (*AQK*).

The variability of the inter-station errors with period is shown in Figure 8 for few selected stations. In the top panel, the results for four rock stations (class 0) are illustrated. *S. Marco dei Cavoti* and *Sannicandro Garganico* recorded the Molise earthquake and show completely opposite error distributions for periods smaller that 0.4 s, being over-estimated and under-estimated by the predictions, respectively. These differences could be partially ascribed to the strong lateral seismic attenuation contrast observed in the area (Zolezzi et al., 2008). The authors derived two-dimensional images of the frequency-dependent attenuation structure in Southern Apennines by performing a quality factor (Q) tomography. They observed low Q along the Apennine chain toward the Tyrrhenian sea (see Figure 3 in Zolezzi et al., 2008) and higher values to the east, in correspondence with the Gargano zone. They interpreted this low-attenuation area (with a variation of up to 50% with respect to the average Q) as due to the presence of the high-velocity anomaly of the Apulia carbonate platform (Chiarabba and Amato, 1996). The seismic rays propagates towards *Sannicandro Garganico* through the high Q zone and towards *S.Marco dei Cavoti* in the low Q zone, therefore the difference between the inter-station errors obtained at low periods agrees with a different amount of anelastic attenuation cumulated by seismic rays along the source-to-receiver paths.

Station *Assisi* that recorded the 1997-98 Umbria-Marche sequence, shows positive errors in the range 0.2-0.5 s. Since this station was installed close to San Francis Cathedral, the response of the structure affected the spectral ordinates at these periods. Finally, the errors for *Monte Fiegni* are large and negative over the entire period range, suggesting that this station behaves as bedrock.

In the middle panel of Figure 8 the errors associated to stations belonging to class 1 (thickness of deposits smaller than 20 m) are shown. Three stations (*Vieste, Malcesine* and *Nocera Umbra*) show large positive error (under-estimation) at periods around 0.1 s, suggesting that these sites are affected by strong amplifications in the high frequency range. The amplification for *Nocera Umbra*

is well documented by numerous works (Rovelli et al., 2002; Cultrera et al., 2003) and explained as a buried wedge of weathered rock underlying the station.

In the bottom panel of Figure 8 the errors relevant to the four stations of class 2 (deep alluvium) are shown. Since this class includes stations installed on alluvial basins having very different extension and thickness, the inter-station distribution of error shows a large variability. For example, the sediments below stations *Borgo Ottomila* (Fucino basin, Central Italy) and *Gubbio Piana* are thicker than 500 m and large positive errors are obtained for the period of 2s. Previous studies (e.g. Pacor et al., 2007; Bindi et al. 2009) showed that the site response of *Gubbio Piana* has been strongly influenced by locally generated surface waves that produce significant amplification with respect to a nearby rock site, in the period range from about 0.5 to 2.5s.

Station *Colfiorito* is installed on a alluvial basin much smaller than the Gubbio and Fucino basins, and the sedimentary cover is about 80 m thick. The amplification around 1 Hz for this station is well documented (Di Giulio et al., 2003; Rovelli et al., 2001). Finally, station *Brienza* is installed over 30 m of compact sediments with average velocity of 500 m/s. The characteristics of this station match the requirements of class 2 but they are close to the limit separating class 2 from class 1.The errors shown in Figure 8 suggest that this station is affected by site amplification at about 0.15 s, larger than the average amplification for stations in class 2.

Figure 9 shows the inter-station errors at four selected periods for the three classes. The errors shown in the top panel (T<=0.1 s) are computed by averaging the errors over periods shorter than 0.1 s. At T=2s, stations belonging to class 2 (deep alluvium) show the largest variability that can be ascribed to strong site amplification at periods longer than 1s, affecting the stations installed over sediments cover thicker than 100m, as already shown in Figure 8. The variability persists also for shorter periods, indicating that class 2 is affected by local site amplification over a broad range of periods. The dispersions of the inter-station errors for class 0 (rock) generally increases with decreasing period, while the three classes have the largest dispersion around 0.2 s.

Comparison between error distributions

The previous analyses show that the inter-station errors are larger than the inter-event errors. A further confirmation of this predominance comes from the residual versus residual analysis proposed by Lee et al (1998). This method considers only stations that recorded more than one earthquake. The residuals are corrected for the inter-event component of error and, pairs of records, belonging to the same station, are randomly combined and plotted. If the site effect is the dominant factor in controlling the residuals, then a good correlation between pairs is expected and the residual versus residual plot will follow the diagonal.

Figure 10 (top) shows the results of this analysis for maxPGA and maxPGV. The residuals scatter mainly along the diagonal, with a correlation coefficient of 0.60. Since the number of available pairs is 86 (i.e. 84 degrees of freedom) and the t-Students coefficient is 6.85, the null hypothesis of no correlation among pairs can be rejected even at 1% level of significance. We applied the same approach to detect the inter-event variability. For each earthquake recorded by at least two stations, the residuals are corrected for the inter-station error and, for each earthquake, pairs of records are randomly combined and plotted, as in the previous case. Figure 10 (bottom) shows that the residuals have no clear trend, indicating that significant correlation does not exist, the t-Student is equal to 1.59 and the null hypothesis of no correlation can be rejected only at 10% level of significance.

Comparisons with European equations

The GMPEs developed in this study are used to explore the characteristics of the ground motion variability of the Italian strong-motion data. However, since new empirical GMPEs are obtained for Italy from a limited dataset, we should compare our model with the equations previously derived for Europe (Ambraseys et al., 2005, hereinafter Amb05; Akkar and Bommer, 2007, hereinafter AkBo07) to test their reliability. The attempt of performing a comparison between regional versus global models is beyond the aim of this work. Results on this subject can be found in Stafford et al. (2008) where a comparison between NGA models and European data is shown, and in Douglas (2007) where regional versus global models are discussed.

The comparisons are performed for three different magnitudes (Mw=6.9, 6, and 5), considering Joyner-Boore distance, rock condition and normal-faulting. Figure 11 shows the comparison for maxPGA (left) and maxPGV (right). For Mw= 6.9 and maxPGA, a good agreement with Amb05 is observed (top left panel), although Amb05 shows slightly larger mean values. The standard deviation of Amb05, which decreases with increasing magnitude, is 0.2178 for Mw=6.9 while the standard deviation of the model derived in this study is 0.2963.

The two GMPEs show different behaviours for decreasing magnitude. In particular, the attenuation with distance of Amb05 becomes stronger while the dependence on magnitude of the geometrical spreading is not resolved with this dataset. This is particular evident in the comparison for Mw=5, where the two models agree only in the distance range sampled by the Italian data (from 10 to 30 km). In particular, the failure in describing the influence of magnitude on attenuation can be ascribed to the poor sampling of distances larger than 10 km for the earthquakes with Mw<5.5 in this study (Figure 2), which reduces the significance of the magnitude-dependent geometrical spreading.

For Mw=6 the observations for strike-slip (squares) reverse-slip (triangles) and normal mechanism (dots) have similar values, confirming that the dataset is not sufficient for the detection of differences between fault mechanisms.

In figure 11 (right panels) comparison with AkaBo07 is performed for PGV. For Mw=6.9, AkaBo07 predicts smaller PGV at short distances, and decays less rapidly with distance. The decay with distance is similar for Mw=6, but with larger mean values predicted by AkaBo07. For Mw=5, the predictions of the two models agree only at the distance sampled by Italian data (about 30 km), while for larger distances they differ, as a consequence of a not significant magnitude-dependent geometrical spreading coefficients derived in the present study.

Finally, Figure 12 shows the comparison with Amb05 for the maximum horizontal spectral acceleration (maxSA), considering three magnitudes (5, 6, and 6.9) and two distances (20 and 50 km). For a distance of 20 km (top panel), the agreement between the Amb05 and this study is satisfactory, with a slightly tendency of Amb05 to predict larger acceleration for periods smaller than 0.2 s. When distance increases to 50 km, a good match is observed for magnitudes greater than 6, while the spectral accelerations predicted in this study for magnitude 5 over-estimate those predicted by the Amb05 model. These results confirm that the main difference with the European model lies in the magnitude dependence of the geometrical spreading.

Comparison with Italian GMPE

The GMPEs calibrated in this study are also compared to the empirical models previously developed for Italy (Sabetta and Pugliese, 1996). These models were calibrated considering 95 waveforms recorded at 62 stations corresponding to 17 earthquakes occurred before 1985, in the magnitude range from 4.6 to 6.8 (Ml or Ms) and valid for epicentral or Joyner-Boore distances up to 100km. The SP96 dataset is a subset of the records used for this study and some of the event and the station metatada have been revised within the S6 project. Figure 13 shows the comparisons with SP96 for maxPGA (right panels) and maxPGV (left panels). In general, SP96 have smaller standard deviations, which underestimate the observed ground motion variability (e.g. Scherbaum et al., 2004). For larger magnitudes (M > 6) SP96 overestimates the mean PGA obtained from this study.

The larger PGA values predicted by SP96 could be ascribed to a misclassification of several stations in SP96 (Table 2) and to the different fault geometries used for computing the Joyner-Boore distance (Bindi et al.; 2009). When the magnitude decreases, the match between the mean values improves and a good agreement is observed for Mw=5. For all magnitudes, the decay with distance is similar for the two models.

Differentely from maxPGA, the agreement between SP96 and this study for maxPGV and Mw=6.9. The misclassification of rock sites, actually located on shallow alluvium, that causes an overestimation of PGA , does not affect PGV. For Mw=6, the mean SP96 is between the mean and the mean plus one σ of this study, while for Mw=5 the mean values of the two equations cross between 10 and 20 km.

Finally, in Figure 14 the maxPGA predicted by this study is compared to the value computed accordingly to models developed for two Italian regions, the Umbria-Marche (Bindi et al., 2006) and the Molise regions (Luzi et al., 2006). Since the regional models were calibrated for the hypocentral distance, we have developed a model for maxPGA considering the hypocentral distance as explanatory variable. Since the hypocentral distance accounts for the depth of the earthquake source, we excluded from equation (1) the pseudo-depth parameter *h*. The coefficients ($a,b_1,b_2,c_1,c_2,e_1,e_2,e_3$) obtained for maxPGA are (3.4192,0.4672,0.1231,-1.2221,-0.1643,0, 0.2474, 0.1435).

The analysis of the inter-event errors (Figure 5) highlights the anomalous behaviour of the Molise region, as already observed in several previous studies (e.g., Luzi et al., 2006; Douglas, 2007). The horizontal PGAs predicted by the regional GMPE for the Molise area (Luzi et al., 2006) underestimate by a factor three those predicted by this study, as shown in Figure 13. Opposite results trends are detectable for the vertical component: at 5 km similar vertical PGA are obtained using Luzi et al. (2006) or this study, while the two models diverge when distance increase, being the 50 km vertical PGA of Luzi et al. (2006) two times larger than the values predicted in this study. Latorre et al. (2008) demonstrated that in the Molise area the observed vertical PGV and PGA are generally associable to S-to-P converted waves during propagation. They analysed the recordings of a temporary network installed in the Molise sequence epicentral area, to reconstruct the seismic image of the Apulea Carbonate platform top by migrating and stacking the S-to-P transmitted energies. These analyses confirmed a polarization of the S-to-P energy on the vertical plane.

Figure 14 also compares the predictions made using a regional model valid for the Umbria Marche area (UMA05) (Bindi et al., 2006), characterized by an extensional tectonic regime. A good agreement is observed between UMA05 and this study, confirming the suitability of our model in describing normal-fault earthquakes. The consideration made above confirm the importance of exploiting regional datasets to derive predictive models for limited areas that could be used for deterministic hazard seismic assessment and for the generation of shake maps.

Conclusions

An updated on-line database of strong motion data recorded in Italy was recently available (ITACA; Luzi et al., 2008) for the distribution of waveforms and the dissemination of the metadata relevant to both stations and earthquakes (see Data and Resource Section).

We selected 27 earthquakes within the ITACA dataset, recorded by 146 stations subdivided into three classes based on geology and deposit thickness (rock, shallow and deep alluvium), following the scheme proposed by Sabetta and Pugliese (1987; 1996). In order to explore the inter-event and inter-station variability of this data set, we developed new empirical ground motion prediction equations for PGA, PGV and 5% damped spectral acceleration, considering both the geometric mean and the larger between horizontal components, as well as the vertical one. The adopted functional form takes into account a quadratic term in magnitude and a magnitude-dependent attenuation term, style of faulting and site classification. The GMPEs found in this study do not allow to reproduce the magnitude dependence of the geometrical spreading, due to the limited data set. However there is an acceptable agreement with the main European GMPEs (Akkar and Bommer, 2007; Ambreseys et al.; 2005), for distances shorter than 100km and moderate magnitudes. A remarkable difference is found with the GMPE generally used for Italy (Sabetta and Pugliese, 1996) in terms of standard deviation, which increases up to about 0.3.

Regressions were performed adopting the random effect model, with the aim of isolating the inter-event and the inter-station components of variance. For periods up to 0.35s the largest component of variability is carried out by the inter-station variability ($\sigma_{station}$ in Tables from 6 to 8) while, for longer periods, the inter-event, inter-station and record-to-record variances are similar, with a slightly dominance of the record-to-record variance.

For the maximum horizontal PGA the inter-station error reaches values up to 0.4, while most of the inter-event errors are acceptable and vary in the range from -0.2 and 0.2. The error distribution analysis also allows the detection of earthquakes and stations with significant deviation from the average, caused by the strong over-estimation or underestimation of the predictions (i.e. Molise 2002 and Sicily 1990 among the events).

The residual analysis also confirm that the dominant component of variance is mainly related to the inter-station component. Douglas and Gehl (2008) reached the same conclusions after analyzing few recordings of the Molise and Umbria-Marche sequences, attributing the vast majority of the observed variance to un-modelled site effects.

Our results agree with the statement by Akkar and Bommer (2007) "*it is important to point out that the geotechnical information available on most European strong-motion recording stations is very limited and the classifications are often based on little more than descriptions of the surface*

geology. Many efforts are currently underway in Europe to improve the site classification of strong-motion accelerograph stations". The ITACA database contains a poor site characterization as well, since only the 6% of the 600 stations are qualified by a shear wave velocity profile. Further efforts are currently spent in Italy to achieve an acceptable level of geotechnical characterization. A new project (INGV-DPC *S4* Project 2007-2009) has been funded to improve the geophysical and geotechnical characterization of sites where the strong motion stations are installed. The improvement of knowledge on site conditions should also lead to new site classifications schemes finalised to ground-motion prediction estimations. The large dispersion affecting the inter-station distribution of error suggests, in fact, that alternative classification scheme, based on parameters such as depth of the soil deposit (H), average shear wave velocity down to depth H ($V_{s,H}$), the resonance period (T_0), should be determined in order to reduce the inter-station variability. The analysis of inter-event and inter-station errors, as proposed in this study, could be useful to check new classification effectiveness.

Data and Resources Section

The strong ground motion data used in the present article can be down-loaded from the ITACA database: http://itaca.mi.ingv.it (last accessed on 28 July, 2008). All the information about the database are included in the Deliverables of the project "*Italian strong-motion database relevant to the period 1972-2004*", available on-line at http://esse6.mi.ingv.it/ (last accessed on 28 July, 2008). In particular, we used Deliverables 5 and 6.

Moreover, the following data resources has been considered in this article:

Castello, B., G. Selvaggi, C. Chiarabba and A. Amato (2006). CSI Catalogo della sismicità italiana 1981-2002, versione 1.1. INGV-CNT, Roma. http://www.ingv.it/CSI/

DISS Working Group (2006). Database of Individual Seismogenic Sources (DISS), Version 3.0.2: A compilation of potential sources for earthquakes larger than M 5.5 in Italy and surrounding areas. http://www.ingv.it/DISS/, © INGV 2005, 2006 - Istituto Nazionale di Geofisica e Vulcanologia - All rights reserved.

SSN – Monitoring System Group (2002), The strong motion Records of Umbria-Marche Sequence (September 1997–June 1998), CD-ROM.

Dipartimento della Protezione Civile—Ufficio Servizio Sismico Nazionale—Servizio Sistemi di Monitoraggio (2004). The Strong Motion Records of Molise Sequence (October 2002–December 2003), CD-ROM, Rome.

Acknowledgements

We wish to acknowledge F.Sabetta for his suggestions and the Italian Department of Civil Protection for providing the funds that allowed the fulfilment of the strong-motion database. Many authors contributed to the achievement of this work and the link to the S6 project (see Data and Resource Section) provides the list of the working group. Constructive comments from the Associate Editor G. Atkinson, and an anonymous reviewer are gratefully acknowledged.

References

Abrahamson, N. A., and R. R. Youngs (1992). A stable algorithm for regression analyses using the random effects model, *Bull. Seism. Soc. Am.* **82,** 505–510.

Akkar, S. and JJ., Bommer (2007). Empirical prediction equations for peak ground velocity derived from strong-motion records from Europe and the Middle East. Bull. Seism. Soc. of Am, 97, 511-530, DOI: 10.1785/0120060141.

Ambraseys, N. N., J. Douglas, S. K. Sarma, and P. M. Smit (2005). Equations for estimation of strong ground motions from shallow crustal earthquakes using data from Europe and Middle East: Horizontal peak ground acceleration and spectral acceleration, *Bull. Earthquake Eng.*, 3, 1– 53.

Atkinson, G. M. (2006). Single-station sigma. *Bull Seism Soc Am,* **96**,446 -455

Basili, R., G. Valensise, P. Vannoli, P. Burrato, U. Fracassi, S. Mariano, M.M. Tiberti, and E. Boschi (2008). The Database of Individual Seismogenic Sources (DISS), version 3: summarizing 20 years of research on Italy's earthquake geology, *Tectonophysics,* 453, 20-43

Bindi, D., L. Luzi, F. Pacor, G. Franceschina, and R. R. Castro (2006). Ground-motion predictions from empirical attenuation relationships versus recorded data: the case of the 1997–1998 Umbria-Marche, Central Italy, strong-motion data set, *Bull. Seism. Soc. Am.* **96**, 984-1002.

Bindi, D., S. Parolai, H. Grosser, C. Milkereit, and E. Durukal (2007). Empirical ground-motion prediction equations for northwestern Turkey using the aftershocks of the 1999 Kocaeli earthquake. Geoph. Res. Let., **34**, L08305. DOI: 10.1029/2007GL029222.

Bindi, D., Parolai, S. F. Cara, G. Di Giulio, G. Ferretti, L. Luzi, G. Monachesi, F. Pacor, and A. Rovelli (2009). Site amplifications observed in the Gubbio Basin, Central Italy: hints for lateral propagation effects, *Bull. Seism. Soc. Am.* in press

Bindi, D., L. Luzi, F. Pacor, F. Sabetta and M. Massa (2009). Towards a new reference ground motion prediction equation for Italy: update of the Sabetta-Pugliese (1996), accepted on *Bull Earthquake Eng*

Boschi, E., D. Pantosti, D. Sliejko, M. Stucchi and G. Valensise (1993). Irpinia 10 anno dopo, special issue on the meeting, Sorrento, Novembre 19-24, 1990, Annali di Geofisica, XXXVI.

Brillinger, D. R., and H. K. Preisler (1985). Further analysis of the Joyner-Boore attenuation data. *Bull. Seism. Soc. Am.*. 75, 611–614.

Castro, R.R., M. Mucciarelli, G. Monachesi, F. Pacor, and R. Berardi (1999). A review of nonparametric attenuation functions computed for different regions of Italy, Annali di Geofisica, 42, 735-748.

Castro, R.R., Pacor, F., Bindi D., Franceschina G., and Luzi, L. (2004), Site response of strong motion stations in the Umbria region, Central Italy, Bull. Seismol Soc. Am. 94, 576–590.

Chen, Y.-H., and C.-C. P. Tsai (2002). A new method for estimation of the attenuation relationship with variance components. Bull. Seismol. Soc. Am. 92,1984 -1991

Chiarabba, C., and A. Amato (1996). Crustal velocity structure of the Apennines (Italy) form P-waves travel time tomography, Annali di Geofisica, 39, 1133-1148.

Cultrera, G., Rovelli, A., Mele, G., Azzara, R., Caserta, A., And Marra, F. (2003), Azimuth dependent Amplification of Weak and Strong Ground Motions within a Fault Zone (Nocera Umbra, Central Italy), *J. Geophys. Res.* 108 (B3), 2156, doi:10.1029/2002JB001929.

Di Bona, M., M. Cocco, A. Rovelli, R. Berardi, and E. Boschi (1995). Analysis of strong-motion data of the 1990 Eastern Sicily earthquake, Annali di Geofisica 38, 283--300.

Di Giulio, G., A. Rovelli, F. Cara, R. M. Azzara, F. Marra, R. Basili, and A. Caserta (2003), Long-duration asynchronous ground motions in the Colfiorito plain, central Italy, observed on a two-dimensional dense array, *J. Geophys. Res.*, *108*(B10), 2486, doi:10.1029/2002JB002367.

Douglas J (2007). On the regional dependence of earthquake response spectra. ISET J Earthq Technol, 44, 71–99

Douglas, J., and P. Gehl (2008). Investigating strong ground-motion variability using analysis of variance and two-way-fit plots, *Bull. Earthquake Eng.*, doi: 10.1007/s10518-008-9063-8

Efron, B. and R. J., Tibshirani (1994). An Introduction to the Bootstrap. Chapman & Hall/CRC, pp 456, ISBN 978-0412042317.

Latorre D., P. De Gori, C. Chiarabba, A. Amato, J. Virieux, and T. Monfret (2008). Three-dimensional kinematic depth migration of converted waves: application to the 2002 Molise aftershock sequence, Geophysical Prospecting, 56, 587-600.

Laurenziano, G., and E. Priolo (2005). Numerical modeling of the 13 December 1990 M 5.8 East Sicily earthquake at the Catania accelerometric station, *Bull Seism Soc Am*, 95, 241-251; DOI: 10.1785/0120030126

Lee, Y., Y. Zeng, and J. G. Anderson (1998). A simple strategy to examine the sources of errors in attenuation relations, *Bull Seism Soc Am*.; 88, 291 - 296

Luzi, L., D. Bindi, G. Franceschina, F. Pacor, And R. R. Castro (2005) Geotechnical Site Characterisation in the Umbria-Marche Area and Evaluation of Earthquake Site-Response. *Pure Appl. Geophys*. 162, 2133–2161.

Luzi L., Morasca P., Zolezzi F., Bindi D., Pacor F., Spallarossa D., and Franceschina G., (2006) Ground motion models for Molise region (Southern Italy), *First European Conference on*

Earthquake Engineering and Seismology (a joint event of the 13th ECEE & 30th General Assembly of the ESC) Geneva, Switzerland, 3-8 September.

Luzi L., Hailemikael S., Bindi D., Pacor F., Mele F., Sabetta F. (2008). ITACA (ITalian ACcelerometric Archive): a Web Portal for the Dissemination of the Italian Strong Motion Data. Submitted to Seism. Res. Letters., 79, 716-722

Malagnini, L., and K. Mayeda (2008). High-stress strike-slip faults in the Apennines: an example from the 2002 San Giuliano earthquakes (southern Italy), *Geophys Res Lett*, 35, L12302, doi: 10.1029/2008GL034024

Mele F., Badiali L., Marcocci C. and Piscini A. (2002). Locator: i codici. Un sistema di localizzazione in tempo quasi reale. Technical notes of Centro Dati e Informazione sui Terremoti n. 6 / 2002.

Morikawa, N., T. Kanno, A. Narita, H. Fujiwara, T. Okumura, Y. Fukushima, and A. Guerpinar (2008). Strong motion uncertainty determined from observed records by dense networks in Japan. .*J Seismology* 12, 529-546. doi:10.1007/s10950-008-9106-2

Pacor, F., D. Bindi, L. Luzi, S. Parolai, S. Marzorati, and G. Monachesi (2007). Characteristics of strong ground motion data recorded in the Gubbio sedimentary basin (Central Italy), *Bull Earthquake Eng* 5:27-43, DOI 10.1007/s10518-006-9026-x.

Pondrelli, S., S. Salimbeni, G. Ekström, A. Morelli, P. Gasperini and G. Vannucci (2006). The Italian CMT dataset from 1977 to the present, *Phys. Earth Planet. Int*., , **159**, 286-303, doi:10.1016/j.pepi.2006.07.008

Power M, Chiou B, Abrahamson N, Roblee C (2006). The "Next Generation of Ground Motion Attenuation Models" (NGA) project: an overview. In: Proceedings of the 8th U.S. national conference on earthquake engineering, San Francisco, CA, Paper No. 2022

Rovelli, A., Scognamiglio, L.,Marra, F., and Caserta, A. (2001), Edge-diffracted 1-sec Surface Waves Observed in a Small-size Intramountain Basin (Colfiorito, Central Italy), *Bull. Seismol. Soc. Am.* **91**, 1851–1866.

Rovelli A., Caserta A., Marra F., and V. Ruggiero (2002). Can Seismic Waves Be Trapped inside an Inactive Fault Zone? The Case Study of Nocera Umbra, Central Italy. *Bull. Seism. Soc. Am.*, **92**, 2217-2232.

Sabetta, F. and A. Pugliese (1987). Attenuation of peak horizontal acceleration and velocity from Italian strong-motion records, *Bull Seism. Soc. Am.* **77**, 1491-1513.

Sabetta, F., and A. Pugliese (1996). Estimation of response spectra and simulation of nonstationary earthquake ground motions, *Bull Seism. Soc. Am.* **86**, 337 - 352.

Sano`, T., Pugliese, A., Romeo, R. W., And Marsan, P. (1998), Effetti locali a Cesi (Pg) durante la sequenza sismica del settembre ottobre 1997, Ingegneria sismica, Anno XV, 3, 14–20.

Scherbaum, F., F. Cotton, and P. Smit (2004). On the use of response spectral-reference data for the selection and ranking of ground-motion models for seismic-hazard analysis in regions of moderate seismicity: the case of rock motion, *Bull. Seism. Soc. Am.* **94,** 2164–2185.

Spudich, P., W. B. Joyner, A. G. Lindh, D. M. Boore, B. M. Margaris, and J. B. Fletcher (1999). SEA99: A revised ground motion prediction relation for use in extensional tectonic regimes, *Bull. Seism. Soc. Am.* **89**, 1156-1170

Stafford, P. J., F. O. Strasser, and J. J. Bommer (2008). An evaluation of the applicability of the NGA models to ground-motion prediction in the Euro-Mediterranean region. *Bull Earth Engineering* **6** ,149 -177.

Strasser, F., N.A. Abrahmson, and J.J. Bommer (2009). Sigma: Issues, Insights, and Challenges, Seism. Res. Lett., 80, 40-56; DOI: 10.1785/gssrl.80.1.40

Vannucci G., and P. Gasperini (2004). The new release of the database of Earthquake Mechanisms of the Mediterranean Area (EMMA version 2). Annals of Geophysics, supplement to vol.47, N. 1

Zolezzi, F., P. Morasca, K. Mayeda, W. S. Phillips, and C. Eva (2008). Attenuation tomography of the Southern Apennines (Italy), *Journal of Seismol*, 12, 355-365, , DOI 10.1007/s10950-007-9079-6

Figure Captions

Figure 1. Stations (right) and earthquakes (left) considered in the present study.

Figure 2 Moment magnitude versus fault-distance scatter-plot. The color of the symbol represents the soil class (white: rock ; black: shallow alluvium ; grey: deep alluvium).

Figure 3 PGA (top) and PGV (bottom) versus Joyner-Boore distance for two magnitudes (4.5 and 6.9) and three components of motion: maximum horizontal (black line), average horizontal (grey line) and vertical (dashed line).

Figure 4 a) Residuals, computed as $\log_{10}$(observation/prediction), for maxPGA. b) The same as a) but here the residuals are corrected for the inter-event error. c) The residuals of panel a) are shown against magnitude. d) The same as c) but against fault distance. Different symbols represent different style of faulting conditions: normal-slip (squares), reverse-slip (triangles) and strike-slip (circles).

Figure 5 Inter-event distribution of error for maxPGA. The Event ID corresponds to identification number (eveID) of the earthquakes listed in Table 1.

Figure 6 Inter-event distribution of error for spectral acceleration. The results are shown for subset of earthquakes (see Table 1), divided accordingly to their style of faulting.

Figura 7 Inter-station distribution of error for maxPGA. The codes indicate the name of some stations (CMM: Castiglione Messer Marino, AQK: L'Aquila-Valle Aterno Aquil-parking; SCV: S.Marco dei Cavoti; ANC: Ancona; CAT: Catania Piana; LCT: Licata; NOT: Noto; PCH: Pachino; PTL: Pietralunga. SCF: Scafa; VZZ: Vizzini).

Figure 8 Inter-station distribution of error for the maximum horizontal spectral acceleration at four different periods (0.2, 0.3, 1 and 2 s). The top panel shows the inter-station errors averaged over the periods <=0.1s. Different symbols represent different soil classes: rock (squares), shallow alluvium (triangles) and deep alluvium (circles).

Figure 9 Inter-station distribution of error for the maximum horizontal spectral acceleration at four different periods (0.2, 0.3, 1 and 2 s). The top panel shows the inter-station errors averaged over the periods <=0.1s. Different symbols represent different soil classes: rock (squares), shallow alluvium (triangles) and deep alluvium (circles).

Figure 10 Residual-residual plot proposed by Lee et al. (1998) (see text for explanation). Top panel: the residuals are corrected for the inter-event errors; bottom panels: the residuals are corrected for the inter-station errors. The results for both the maximum horizontal PGA (left) and PGV (right) are shown.

Figure 11 Mean maxPGA ± one σ (left) and Mean maxPGV ± one σ (right) versus Joyner-Boore distance for three magnitudes, considering rock site and normal fault conditions. The results from this study are compared to Ambraseys et al, 2005, Amb05 for maxPGA and Akkar and Bommer, 2007, AkBo07 for maxPGV. The black circles are observed peak values. For Mw=6, observed peak values for thrust (triangles) and strike-slip (squares) earthquakes are also shown.

Figure 12 Spectral accelerations (SA) versus periods predicted by this study (ITA07, black line) and by Ambraseys et al. (2005) (Amb05, grey line)), for two fault-distances (20 km in the top panel and 50 km in the bottom one), and three different magnitudes.

Figure 13 Mean maxPGA ± one σ (Left) and mean maxPGV ± one σ (right) versus Joyner-Boore distance for three magnitudes, considering rock site compared to the Sabetta and Pugliese, 1996, SP96.

Figure 14. Comparison among the PGA versus distance for a magnitude 5.7 earthquake, considering the Molise model of Luzi et al, 2006 (dashed lines), the UMA05 model, derived by Bindi et al., 2006 (dotted line) for the 1997 Umbria-March sequence, and this study (continuous lines). The black lines represent the results for the maximum horizontal component, the grey lines those for the vertical one.

Table 1. Earthquakes used in this study**.**

Eve Id	Date	Name	Latitude	Longitude	Depth [km]	ML	Mw	M_{SP87}*	NR	NR_{SP87}
1	1972-06-14 18:55:46	Ancona	43.65	13.60	3	4.7	4.8		2	-
2	**1976-05-06 20:00:12**	Friuli 1st shock	46.35	13.26	12	6.4	6.4	6.5	10	8
3	1976-05-09 00:53:44	Friuli	46.22	12.13	20	5.5	5.1	5.3	3	3
4	1976-05-11 22:44:00	Friuli	46.29	12.99	13	5.3	5.0	4.8	4	4
5	**1976-09-11 16:31:11**	Friuli	46.29	13.18	10	5.5	5.2	5.1	4	4
6	**1976-09-11 16:35:01**	Friuli	46.30	13.31	9	5.8	5.6	5.6	6	6
7	1976-09-15 03:15:18	Friuli	46.30	13.19	2	6.1	5.9	6.0	6	4
8	1976-09-15 04:38:53	Friuli	46.26	13.16	21	4.8	4.8**	4.7	3	2
9	**1976-09-15 09:21:18**	Friuli	46.30	13.18	21	6.0	6.0	5.9	10	8
10	**1977-09-16 23:48:08**	Friuli	46.28	12.98	21	5.3	5.3	5.2	5	4
11	**1978-04-15 23:33:47**	Sicily	38.26	15.11	22	5.5	6.0	5.8	4	4
12	**1979-09-19 21:35:36**	Valnerina	42.80	13.04	6	5.5	5.8	5.8	8	5
13	**1980-11-23 18:34:53**	Irpinia	40.76	15.30	15	6.5	6.9	6.8	20	17
14	1980-12-01 19:04:29	Irpinia	40.88	15.30	9	4.6	4.6**	4.6	11	4
15	**1981-01-16 00:37:47**	Irpinia	40.83	15.44	10	4.6	5.2	4.7	12	8
16	**1984-04-29 05:02:59**	Gubbio	43.20	12.56	6	5.2	5.6	5.6	6	5
17	**1984-05-07 17:49:42**	Lazio-Abruzzo	41.70	13.86	20	5.9	5.9	5.8	14	7
18	**1984-05-11 10:41:50**	Lazio-Abruzzo	41.78	13.88	12	5.7	5.5	5.4	9	2
19	**1990-05-05 07:21:22**	Potenza	40.64	15.86	10	5.2	5.8		5	-
20	**1990-12-13 00:24:29**	East Sicily	37.27	15.32	7	5.4	5.6		8	-
21	**1997-09-26 00:33:12**	Umbria-Marche 1st shock	43.02	12.89	3	5.6	5.7		15	-
22	**1997-09-26 09:40:26**	Umbria-Marche 2nd shock	43.01	12.85	10	5.8	6.0		21	-
23	1997-10-14 15:23:10	Umbria-Marche 3rd shock	42.89	12.89	7	5.5	5.6		25	-
24	1998-09-09 11:28:00	Pollino	40.06	15.94	29	5.6	5.6		5	-
25	2002-09-06 01:21:28	Southern Tyrrhenian	38.38	13.65	27	5.6	5.9		4	-
26	2002-10-31 10:32:59	Molise 1st shock	41.71	14.89	25	5.4	5.7		12	-
27	2002-11-01 15:09:01	Molise 2nd shock	41.74	14.84	21	5.3	5.7		10	-

(*) = M_S for magnitudes greater or equal to 5.5, M_L for magnitudes lower than 5.5 (Sabetta and Pugliese, 1987). (**) Assumed to be equal to M_L. The earthquakes included in the European database are shown in bold.

Table 2: re-classification for the stations used in the SP87 (* recorded the Mw 6.9 Irpinia earthquake)

Station name	**SP87 class**	**This work**	**Type of estimate**
Benevento*	2	1	Cross-hole
Brienza*	1	2	Cross-hole
Cairano 1	0	1	Geologic map + HVSR
Contrada Fiumicello	0	1	Geologic map + HVSR
Gioia Sannitica*	2	1	Geologic map + HVSR
Messina	0	1	Geologic map + HVSR
Monselice	0	1	Geologic map + HVSR
Nocera Umbra	0	1	Down-hole
Ortucchio	2	1	Geological map
Patti	1	2	Geologic map + HVSR
Pontecorvo	2	1	Geologic map+ HVSR
Roccamonfina*	2	0	Geologic map + HVSR
Tregnago	0	1	Geologic map + HVSR
Vieste*	0	1	Cross – hole

Table 3. Regression coefficients (equation 1) for spectral acceleration (cm/s^2) at different periods, PGA (cm/s^2), and PGV (cm/s), considering the maximum horizontal component.

T[s]	a1	b1	b2	c1	c2	h	e2	e3	f2	f3
0.03	3.4419±0.2789	0.0632±0.2506	0.0851±0.0763	-1.2645±0.1748	0.0533±0.2009	11.0123±3.2119	0.2676±0.0479	0.1462±0.0497	-0.0712±0.0734	0.0304±0.0467
0.04	3.5326±0.3099	0.0791±0.2703	0.0780±0.0757	-1.2979±0.1884	0.0486±0.2071	10.9946±3.7556	0.2653±0.0526	0.1432±0.0508	-0.0723±0.0786	0.0315±0.0478
0.07	3.8932±0.3953	0.0445±0.3248	0.0558±0.0804	-1.4194±0.2341	0.0721±0.2440	13.4672±4.6490	0.2243±0.0577	0.0851±0.0505	-0.0306±0.0834	0.0698±0.0505
0.10	4.2219±0.4508	-0.0413±0.3465	0.0626±0.0711	-1.5337±0.2628	0.1127±0.2518	16.2843±4.6570	0.2634±0.0534	0.0649±0.0485	-0.0479±0.0787	0.0655±0.0462
0.15	4.3128±0.4869	-0.0302±0.3984	0.0461±0.0881	-1.5309±0.2852	0.1247±0.2933	16.5519±5.1797	0.3101±0.0595	0.0842±0.0503	-0.1008±0.0826	0.0244±0.0519
0.20	4.0195±0.4129	0.0615±0.3328	0.0625±0.0856	-1.3711±0.2468	0.0863±0.2507	12.7887±4.6414	0.2749±0.0494	0.1049±0.0496	-0.0850±0.0741	0.0162±0.0498
0.25	3.7518±0.3308	0.1311±0.2978	0.0751±0.0878	-1.2634±0.2056	0.0426±0.2433	10.2919±3.9840	0.2777±0.0546	0.1460±0.0500	-0.0858±0.0676	0.0263±0.0489
0.30	3.5497±0.2591	0.1460±0.2205	0.0719±0.0766	-1.1805±0.1607	0.0507±0.1789	8.5019±3.3076	0.2690±0.0511	0.1669±0.0462	-0.0948±0.0668	-0.0036±0.0510
0.35	3.3163±0.2510	0.2262±0.2420	0.1144±0.0949	-1.0704±0.1634	-0.0080±0.2150	6.7770±3.4401	0.2857±0.0522	0.1917±0.0455	-0.1093±0.0645	-0.0225±0.0535
0.40	3.1773±0.2047	0.2735±0.2138	0.1161±0.0905	-1.0227±0.1382	-0.0265±0.1880	5.5782±2.9038	0.2838±0.0525	0.2156±0.0453	-0.0838±0.0668	-0.0173±0.0533
0.45	3.0778±0.1904	0.2756±0.1994	0.1383±0.0896	-1.0023±0.1295	-0.0289±0.1829	6.0866±2.4595	0.2630±0.0565	0.2688±0.0465	-0.0729±0.0667	-0.0004±0.0565
0.50	2.9647±0.1720	0.3533±0.1907	0.1465±0.0904	-0.9565±0.1191	-0.0763±0.1774	5.2953±2.1212	0.2296±0.0551	0.2884±0.0503	-0.0757±0.0665	0.0140±0.0549
0.60	2.8361±0.1638	0.4360±0.1766	0.1449±0.0938	-0.9346±0.1186	-0.0984±0.1768	3.8025±1.6770	0.1743±0.0550	0.3320±0.0501	-0.0824±0.0698	0.0073±0.0527
0.70	2.7102±0.1498	0.4695±0.1600	0.1336±0.0956	-0.9078±0.1103	-0.0927±0.1637	3.0263±1.2665	0.1269±0.0557	0.3537±0.0522	-0.0873±0.0751	0.0188±0.0509
0.80	2.5937±0.1437	0.5389±0.1586	0.1616±0.0873	-0.8814±0.1029	-0.1375±0.1543	3.0493±1.4449	0.0990±0.0562	0.3718±0.0527	-0.0527±0.0691	0.0255±0.0462
0.90	2.5168±0.1304	0.6010±0.1421	0.1569±0.0787	-0.8794±0.0944	-0.1529±0.1343	2.5793±1.2244	0.0875±0.0547	0.3837±0.0522	-0.0350±0.0756	0.0143±0.0492
1.00	2.4809±0.1274	0.6015±0.1400	0.1482±0.0685	-0.9018±0.0907	-0.1356±0.1222	3.3304±1.3032	0.0960±0.0538	0.3923±0.0538	-0.0165±0.0700	0.0049±0.0493
2.00	2.1233±0.2063	0.5894±0.2282	0.1159±0.0784	-0.9428±0.1298	-0.0354±0.1700	7.7343±3.6456	0.0763±0.0582	0.3524±0.0552	-0.0843±0.0718	-0.0500±0.0523
PGA	3.0761±3.0761	0.1587±0.1587	0.0845±0.0845	-1.0504±-1.0504	-0.0148±-0.0148	7.3469±7.3469	0.2541±0.2541	0.1367±0.1367	-0.0059±-0.0059	0.0168±0.0168
PGV	1.5182±1.5182	0.4821±0.4821	0.1959±0.1959	-0.8536±-0.8536	-0.1686±-0.1686	4.1138±4.1138	0.1670±0.1670	0.2269±0.2269	-0.0155±-0.0155	-0.0064±-0.0064

Table 4. The same as Table 3 but considering the geometrical mean of the horizontal components.

T[s]	a1	b1	b2	c1	c2	h	e2	e3	f2	f3
0.03	3.4206±0.2863	0.0338±0.2578	0.0734±0.0717	-1.2778±0.1756	0.0840±0.1981	11.2842±3.3916	0.2615±0.0486	0.1386±0.0478	-0.0710±0.0715	0.0121±0.0448
0.04	3.5297±0.3025	0.0387±0.2593	0.0671±0.0694	-1.3202±0.1857	0.0827±0.1970	11.6515±3.5321	0.2576±0.0476	0.1323±0.0489	-0.0709±0.0741	0.0162±0.0470
0.07	3.8415±0.4132	0.0319±0.3251	0.0526±0.0767	-1.4182±0.2445	0.0883±0.2396	13.4182±4.6418	0.2223±0.0545	0.0804±0.0521	-0.0250±0.0854	0.0465±0.0465
0.10	4.1747±0.4614	-0.0308±0.3583	0.0560±0.0728	-1.5319±0.2711	0.1165±0.2586	16.5436±4.7234	0.2545±0.0534	0.0560±0.0481	-0.0512±0.0861	0.0578±0.0495
0.15	4.1934±0.4502	-0.0178±0.3916	0.0331±0.0865	-1.4989±0.2673	0.1288±0.2860	15.8024±4.5693	0.3209±0.0565	0.0901±0.0492	-0.1038±0.0842	0.0044±0.0495
0.20	3.8031±0.3665	0.0959±0.2789	0.0494±0.0822	-1.2779±0.2196	0.0799±0.2139	11.3543±4.3647	0.2745±0.0527	0.1007±0.0529	-0.0928±0.0698	-0.0164±0.0474
0.25	3.5748±0.2956	0.1477±0.2413	0.0640±0.0835	-1.1979±0.1824	0.0465±0.1992	9.2337±3.6841	0.2885±0.0515	0.1549±0.0468	-0.1047±0.0632	-0.0196±0.0454
0.30	3.3955±0.2405	0.1582±0.2215	0.0578±0.0808	-1.1338±0.1529	0.0606±0.1866	7.1534±2.9499	0.2814±0.0517	0.1733±0.0455	-0.0790±0.0614	-0.0346±0.0473
0.35	3.1943±0.2231	0.2174±0.2170	0.1168±0.0902	-1.0476±0.1477	0.0034±0.1914	6.2348±3.0269	0.2824±0.0522	0.2054±0.0462	-0.0829±0.0638	-0.0281±0.0497
0.40	3.0893±0.1898	0.2608±0.1913	0.1116±0.0827	-1.0195±0.1286	-0.0070±0.1698	5.3658±2.5178	0.2787±0.0529	0.2280±0.0448	-0.0745±0.0647	-0.0310±0.0517
0.45	2.9845±0.1704	0.2764±0.1841	0.1239±0.0821	-0.9891±0.1156	-0.0085±0.1639	5.3292±2.0728	0.2442±0.0552	0.2671±0.0458	-0.0655±0.0662	-0.0159±0.0552
0.50	2.8706±0.1542	0.3312±0.1815	0.1266±0.0835	-0.9488±0.1059	-0.0394±0.1614	4.6036±2.1189	0.2290±0.0562	0.2972±0.0504	-0.0777±0.0661	-0.0108±0.0547
0.60	2.7214±0.1493	0.4071±0.1610	0.1248±0.0866	-0.9123±0.1070	-0.0613±0.1563	3.3987±1.6175	0.1770±0.0553	0.3416±0.0503	-0.0673±0.0671	-0.0141±0.0496
0.70	2.5781±0.1390	0.4889±0.1475	0.1193±0.0869	-0.8721±0.1039	-0.0902±0.1476	2.4141±1.2249	0.1347±0.0555	0.3604±0.0525	-0.0816±0.0723	0.0020±0.0487
0.80	2.4720±0.1404	0.5459±0.1523	0.1558±0.0789	-0.8530±0.1024	-0.1286±0.1454	2.4479±1.3209	0.1048±0.0539	0.3706±0.0517	-0.0421±0.0731	0.0115±0.0482
0.90	2.4079±0.1267	0.6019±0.1297	0.1469±0.0771	-0.8619±0.0906	-0.1467±0.1258	2.5013±1.2235	0.0999±0.0535	0.3998±0.0476	-0.0200±0.0718	0.0004±0.0473
1.00	2.3597±0.1177	0.6189±0.1330	0.1364±0.0717	-0.8711±0.0838	-0.1416±0.1191	2.8436±1.1139	0.0964±0.0542	0.4000±0.0523	-0.0083±0.0722	-0.0082±0.0461
2.00	2.0670±0.2434	0.6019±0.2252	0.1273±0.0747	-0.9416±0.1487	-0.0566±0.1715	9.0549±4.3384	0.0936±0.0591	0.3627±0.0533	-0.1015±0.0705	-0.0565±0.0531
PGA	3.0191±3.0191	0.1643±0.1643	0.0674±0.0674	-1.0284±-1.0284	-0.0041±-0.0041	6.8963±6.8963	0.2275±0.2275	0.0774±0.0774	-0.0138±-0.0138	0.0005±0.0005
PGV	1.4148±1.4148	0.4507±0.4507	0.1723±0.1723	-0.8268±-0.8268	-0.1348±-0.1348	3.5300±3.5300	0.1832±0.1832	0.2339±0.2339	-0.0369±-0.0369	-0.0343±-0.0343

Table 5. The same as Table 3 but considering the vertical component.

T[s]	a1	b1	b2	c1	c2	h	e2	e3	f2	f3
0.03	3.1402±0.2729	0.3722±0.2475	0.0905±0.0819	-1.2814±0.1736	-0.0872±0.2043	9.8413±3.0956	0.2167±0.0459	0.1175±0.0451	0.0048±0.0697	0.0191±0.0415
0.04	3.2937±0.2657	0.3962±0.2682	0.0916±0.0839	-1.3478±0.1730	-0.1041±0.2162	9.4885±2.6741	0.2235±0.0504	0.1236±0.0460	0.0246±0.0775	0.0343±0.0454
0.07	3.6440±0.3338	0.4114±0.3027	0.0643±0.0887	-1.4592±0.2093	-0.0991±0.2439	10.5360±3.4145	0.2083±0.0499	0.1042±0.0512	0.0943±0.0770	0.0299±0.0483
0.10	3.7793±0.3588	0.3715±0.3070	0.0812±0.0814	-1.4698±0.2226	-0.0836±0.2437	12.1116±3.4911	0.2122±0.0494	0.0671±0.0488	0.0769±0.0737	0.0432±0.0482
0.15	3.7603±0.3891	0.2899±0.3320	0.0537±0.0839	-1.4245±0.2364	-0.0186±0.2601	13.7656±4.1742	0.2496±0.0513	0.0930±0.0470	-0.0336±0.0686	0.0149±0.0455
0.20	3.5443±0.2936	0.3251±0.2798	0.0520±0.0749	-1.3142±0.1824	-0.0436±0.2177	11.6110±3.4321	0.2493±0.0502	0.1037±0.0473	-0.0806±0.0631	-0.0136±0.0510
0.25	3.1244±0.2353	0.3962±0.2143	0.0566±0.0745	-1.1204±0.1531	-0.0744±0.1832	7.6749±2.8760	0.2530±0.0502	0.1281±0.0434	-0.0911±0.0628	0.0136±0.0466
0.30	3.1472±0.2216	0.3439±0.2097	0.1016±0.0765	-1.1595±0.1440	-0.0475±0.1760	8.5486±2.9198	0.2099±0.0482	0.1411±0.0446	-0.0529±0.0574	0.0053±0.0479
0.35	3.0362±0.2350	0.3949±0.2034	0.0957±0.0676	-1.1175±0.1467	-0.0764±0.1644	9.2562±3.4520	0.2137±0.0454	0.1653±0.0429	-0.0774±0.0559	0.0054±0.0463
0.40	2.8359±0.2295	0.3904±0.1823	0.0880±0.0710	-1.0245±0.1463	-0.0664±0.1550	7.1101±3.5280	0.1846±0.0472	0.1630±0.0464	-0.0667±0.0637	0.0240±0.0433
0.45	2.7776±0.2018	0.4052±0.1707	0.0722±0.0713	-1.0029±0.1312	-0.0593±0.1446	6.8317±3.2464	0.1444±0.0473	0.1754±0.0479	-0.0663±0.0680	0.0295±0.0495
0.50	2.6638±0.1750	0.4658±0.1722	0.0782±0.0753	-0.9598±0.1218	-0.0871±0.1546	5.1953±2.4454	0.1196±0.0491	0.1748±0.0455	-0.0686±0.0660	0.0540±0.0471
0.60	2.5220±0.1694	0.5733±0.1697	0.0840±0.0864	-0.9113±0.1233	-0.1165±0.1643	3.8060±1.9741	0.0739±0.0502	0.1699±0.0464	-0.0798±0.0657	0.0318±0.0451
0.70	2.3226±0.1421	0.5412±0.1478	0.0910±0.0833	-0.8178±0.1040	-0.1051±0.1493	2.4878±1.4702	0.0297±0.0468	0.1862±0.0448	-0.0892±0.0656	0.0499±0.0433
0.80	2.2346±0.1613	0.6112±0.1723	0.1217±0.0906	-0.8030±0.1176	-0.1530±0.1724	2.8457±1.8959	0.0489±0.0516	0.2133±0.0458	-0.1204±0.0678	0.0139±0.0464
0.90	2.1894±0.1542	0.6912±0.1598	0.1051±0.0828	-0.8134±0.1096	-0.1831±0.1526	3.5164±1.8689	0.0745±0.0487	0.2237±0.0451	-0.1301±0.0661	0.0003±0.0476
1.00	2.1141±0.1759	0.7480±0.1818	0.0882±0.0902	-0.7928±0.1258	-0.1872±0.1741	3.6107±2.0120	0.0630±0.0486	0.2178±0.0466	-0.1487±0.0667	-0.0120±0.0468
2.00	2.7118±0.4582	0.4015±0.4311	0.0276±0.0841	-1.4321±0.2707	0.1660±0.3021	18.2867±5.3257	0.0281±0.0647	0.2427±0.0612	-0.0795±0.0744	0.0466±0.0689
PGA	3.0421±3.0421	0.3762±0.3762	0.0925±0.0925	-1.2350±-1.2350	-0.0891±-0.0891	9.3012±9.3012	0.1787±0.1787	0.1146±0.1146	-0.0073±-0.0073	0.0222±0.0222
PGV	1.3600±1.3600	0.5978±0.5978	0.1494±0.1494	-0.9636±-0.9636	-0.1618±-0.1618	6.6690±6.6690	0.1543±0.1543	0.2072±0.2072	-0.0934±-0.0934	0.0032±0.0032

Table 6. Inter-event (σ_{event}), inter-station ($\sigma_{station}$), record-to-record (σ_{record}), and total (σ) standard deviations for the maximum horizontal spectral acceleration.

T [s]	σ_{event}	$\sigma_{station}$	σ_{record}	σ
0.0300	0.1532	0.2398	0.1136	0.3064
0.0400	0.1604	0.2484	0.1243	0.3208
0.0700	0.1678	0.2595	0.1307	0.3356
0.1000	0.1484	0.2712	0.1208	0.3319
0.1500	0.1475	0.2664	0.1265	0.3297
0.2000	0.1243	0.2511	0.1564	0.3208
0.2500	0.1610	0.2549	0.1133	0.3221
0.3000	0.1555	0.2084	0.1706	0.3110
0.3500	0.1547	0.2092	0.1676	0.3095
0.4000	0.1620	0.1738	0.2203	0.3240
0.4500	0.1639	0.1609	0.2340	0.3279
0.5000	0.1665	0.1636	0.2376	0.3331
0.6000	0.1838	0.1812	0.2146	0.3357
0.7000	0.2066	0.1692	0.2251	0.3493
0.8000	0.2030	0.1827	0.2078	0.3431
0.9000	0.1851	0.1816	0.2167	0.3379
1.0000	0.1863	0.1953	0.2071	0.3402
2.0000	0.1057	0.1668	0.2697	0.3343
PGA	0.1482	0.2083	0.1498	0.2963
PGV	0.1556	0.1813	0.1996	0.3113

Table 7. The same as in Table 6 but for the geometric mean of the horizontal components.

T[s]	σ_{event}	$\sigma_{station}$	σ_{record}	σ
0.0300	0.1488	0.2311	0.1141	0.2975
0.0400	0.1544	0.2375	0.1230	0.3088
0.0700	0.1624	0.2648	0.0948	0.3248
0.1000	0.1443	0.2768	0.0816	0.3226
0.1500	0.1670	0.2782	0.0791	0.3339
0.2000	0.1230	0.2611	0.1327	0.3177
0.2500	0.1563	0.2293	0.1440	0.3126
0.3000	0.1519	0.2026	0.1679	0.3038
0.3500	0.1497	0.2001	0.1648	0.2993
0.4000	0.1562	0.1800	0.2021	0.3125
0.4500	0.1606	0.1696	0.2205	0.3212
0.5000	0.1639	0.1731	0.2250	0.3278
0.6000	0.1796	0.1883	0.1995	0.3279
0.7000	0.2014	0.1773	0.2095	0.3404
0.8000	0.2000	0.1766	0.2076	0.3381
0.9000	0.1805	0.1740	0.2138	0.3295
1.0000	0.1809	0.1880	0.2024	0.3302
2.0000	0.1280	0.1601	0.2592	0.3305
PGA	0.1465	0.2184	0.1345	0.2930
PGV	0.1529	0.1906	0.1840	0.3059

Table 8. The same as in Table 6 but for the vertical component.

T[s]	σ_{event}	$\sigma_{station}$	σ_{record}	σ
0.0300	0.1293	0.2136	0.1458	0.2891
0.0400	0.1201	0.2322	0.1667	0.3100
0.0700	0.1419	0.2363	0.1572	0.3173
0.1000	0.1420	0.2353	0.1589	0.3174
0.1500	0.1352	0.2247	0.1504	0.3023
0.2000	0.0914	0.2040	0.1831	0.2889
0.2500	0.1094	0.1894	0.1788	0.2825
0.3000	0.1287	0.1818	0.1822	0.2878
0.3500	0.1201	0.1456	0.1911	0.2686
0.4000	0.1241	0.1505	0.1975	0.2775
0.4500	0.1299	0.1577	0.2064	0.2905
0.5000	0.1499	0.1616	0.2032	0.2997
0.6000	0.1634	0.1294	0.2134	0.2983
0.7000	0.1809	0.1133	0.2189	0.3057
0.8000	0.1689	0.1153	0.2309	0.3084
0.9000	0.1564	0.1176	0.2440	0.3128
1.0000	0.1390	0.1362	0.2424	0.3109
2.0000	0.0776	0.2019	0.2712	0.3469
PGA	0.1266	0.2114	0.1394	0.2831
PGV	0.1234	0.1497	0.1963	0.2760

Figure

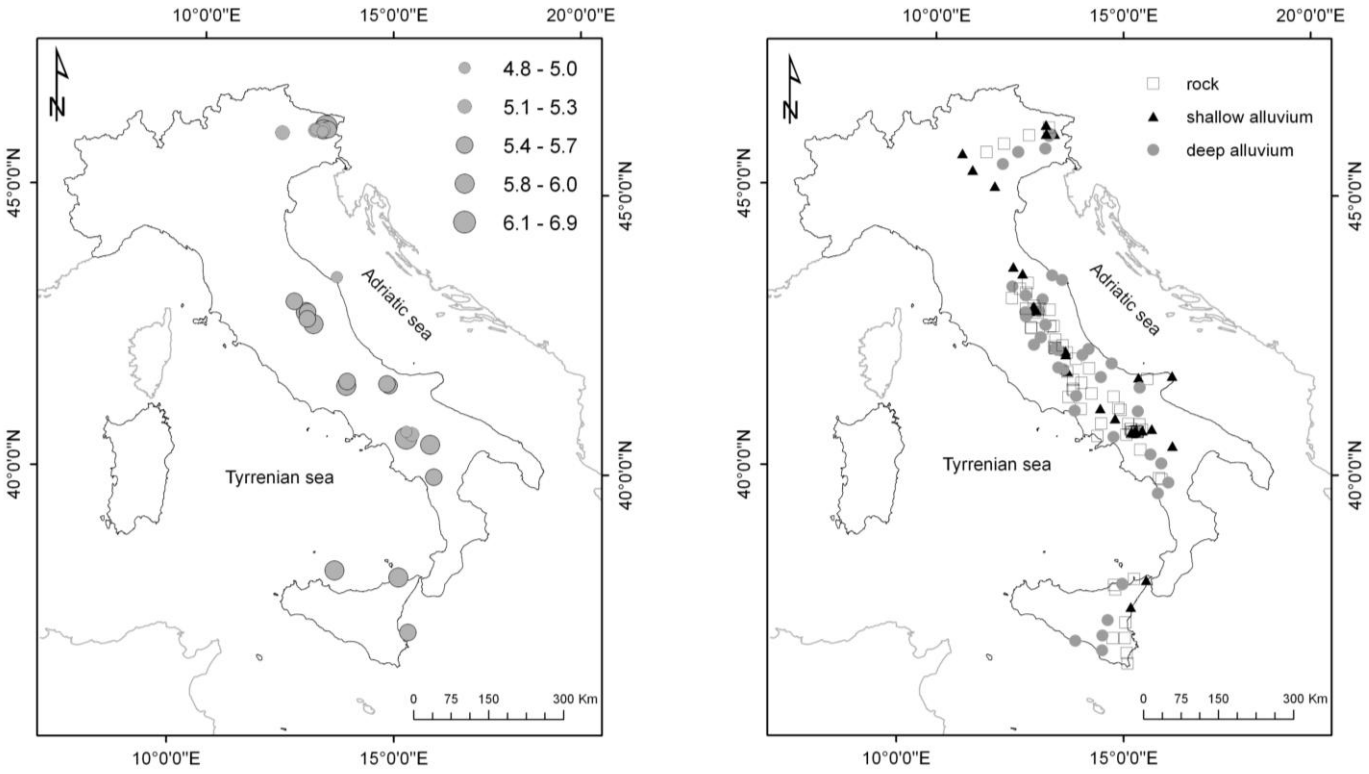

Figure 1

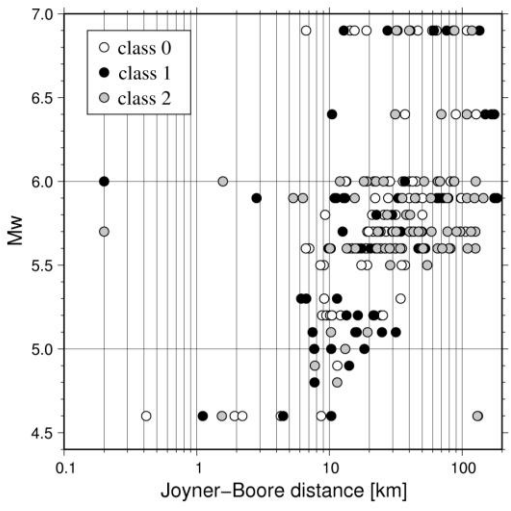

Figure 2

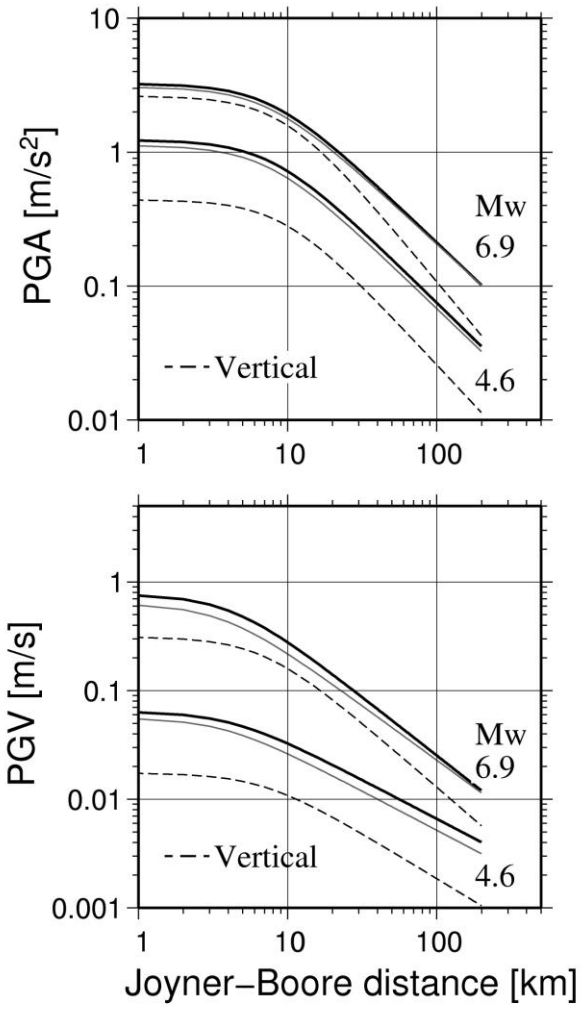
PGA [m/s²]
10
1
0.1
0.01
Mw
6.9
4.6
Vertical
1
10
100
PGV [m/s]
1
0.1
0.01
0.001
Mw
6.9
4.6
Vertical
1
10
100
Joyner–Boore distance [km]

Figure 3

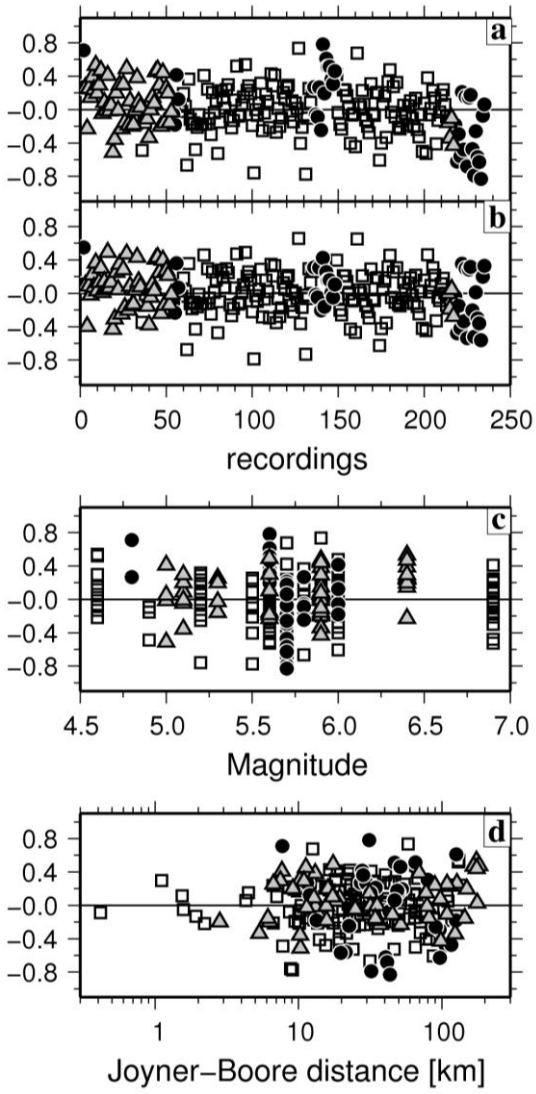
a
b
c
d
0.8
0.4
−0.0
−0.4
−0.8
0
50
100
150
200
250
recordings
4.5
5.0
5.5
6.0
6.5
7.0
Magnitude
1
10
100
Joyner−Boore distance [km]

Figure 4

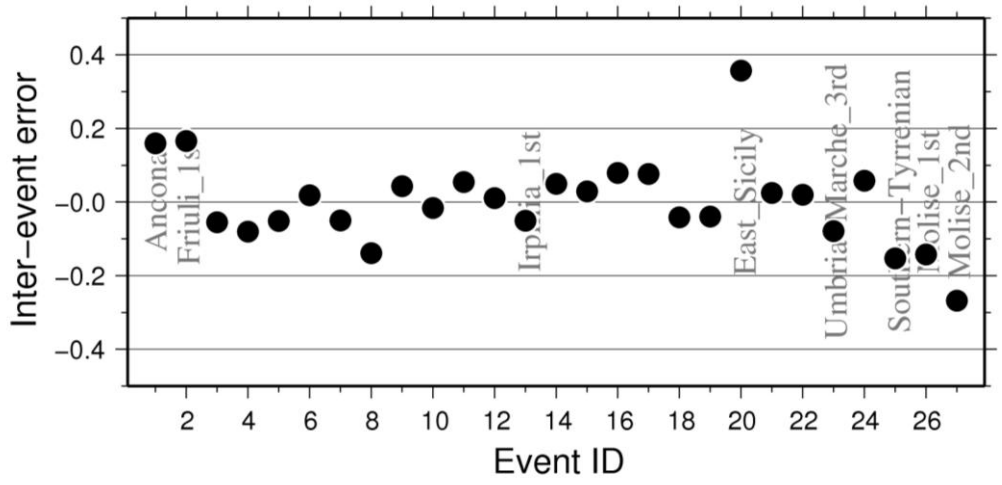
Inter−event error
0.4
0.2
−0.0
−0.2
−0.4
2
4
6
8
10
12
14
16
18
20
22
24
26
Event ID
Ancona
Friuli_1st
Irpinia_1st
East_Sicily
Umbria_Marche_3rd
Southern_Tyrrenian
Molise_1st
Molise_2nd

Figure 5

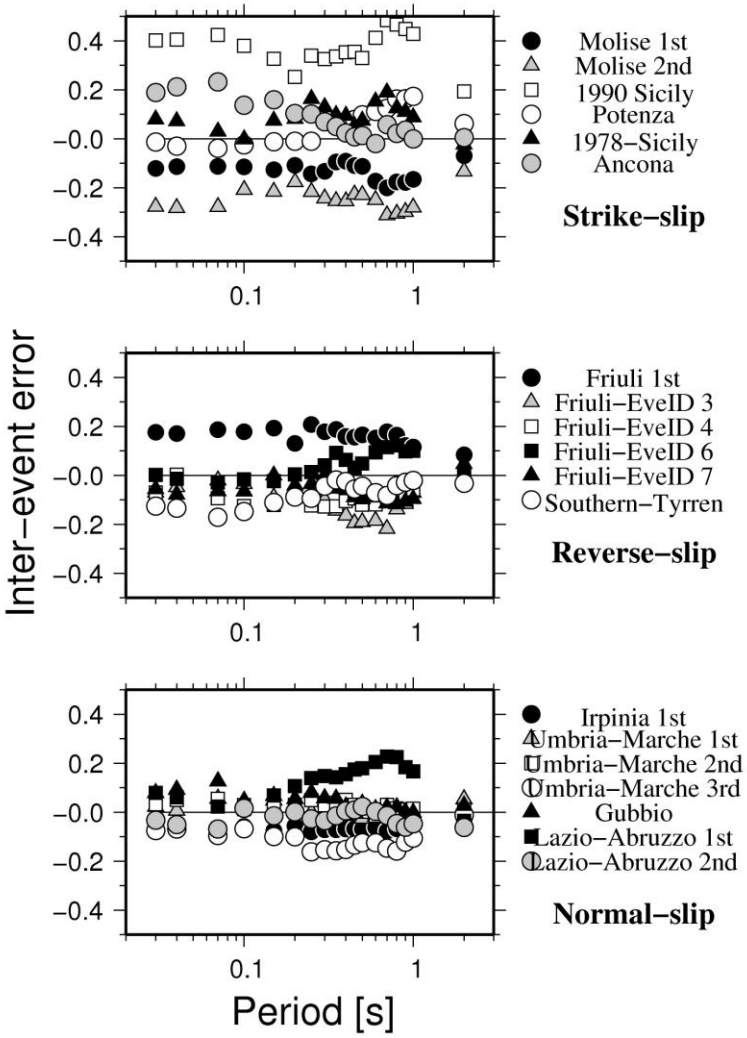
Inter−event error
Period [s]
0.4
0.2
−0.0
−0.2
−0.4
0.1
1
Molise 1st
Molise 2nd
1990 Sicily
Potenza
1978−Sicily
Ancona
Strike−slip
Friuli 1st
Friuli−EveID 3
Friuli−EveID 4
Friuli−EveID 6
Friuli−EveID 7
Southern−Tyrren
Reverse−slip
Irpinia 1st
Umbria−Marche 1st
Umbria−Marche 2nd
Umbria−Marche 3rd
Gubbio
Lazio−Abruzzo 1st
Lazio−Abruzzo 2nd
Normal−slip

Figure 6

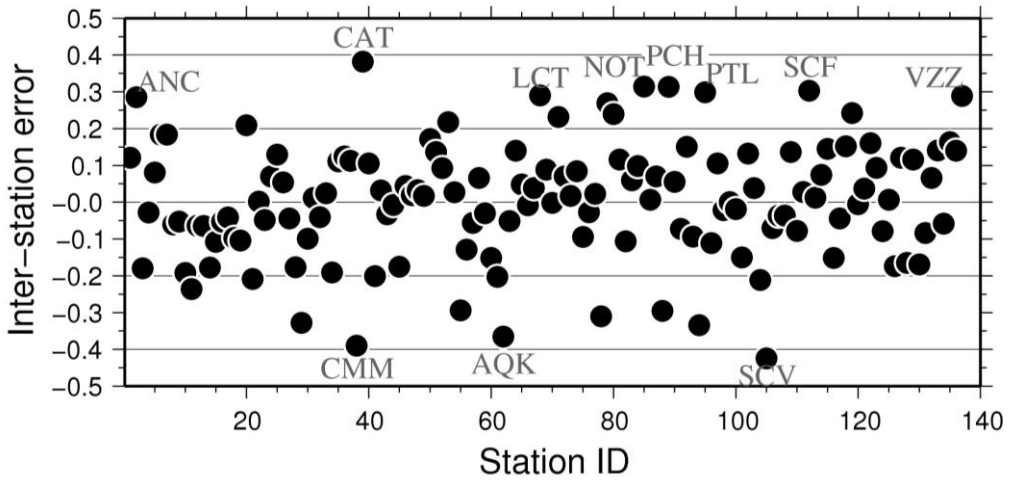
Inter−station error
Station ID
0.5
0.4
0.3
0.2
0.1
−0.0
−0.1
−0.2
−0.3
−0.4
−0.5
20
40
60
80
100
120
140
CAT
ANC
LCT
NOT
PCH
PTL
SCF
VZZ
CMM
AQK
SCV

Figure 7

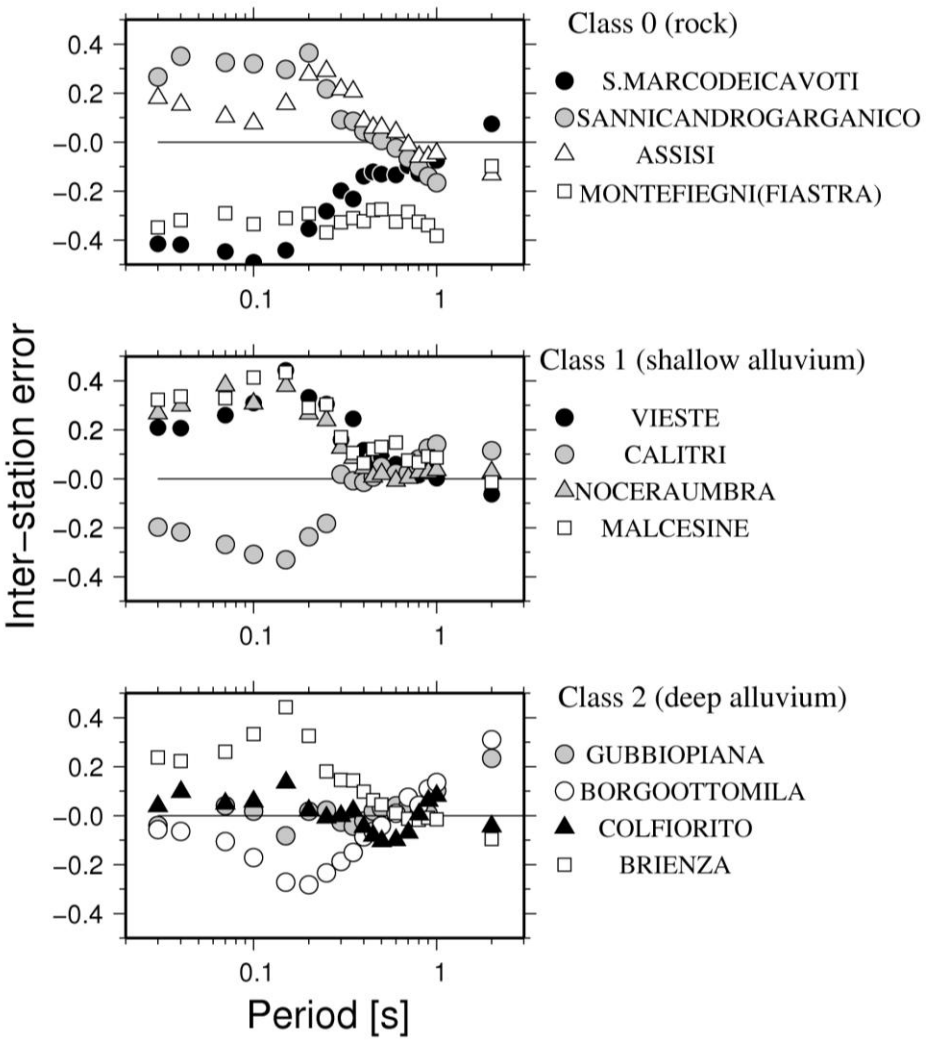
Class 0 (rock)
S.MARCODEICAVOTI
SANNICANDROGARGANICO
ASSISI
MONTEFIEGNI(FIASTRA)
Class 1 (shallow alluvium)
VIESTE
CALITRI
NOCERAUMBRA
MALCESINE
Class 2 (deep alluvium)
GUBBIOPIANA
BORGOOTTOMILA
COLFIORITO
BRIENZA
Inter−station error
Period [s]
0.4
0.2
−0.0
−0.2
−0.4
0.1
1

Figure 8

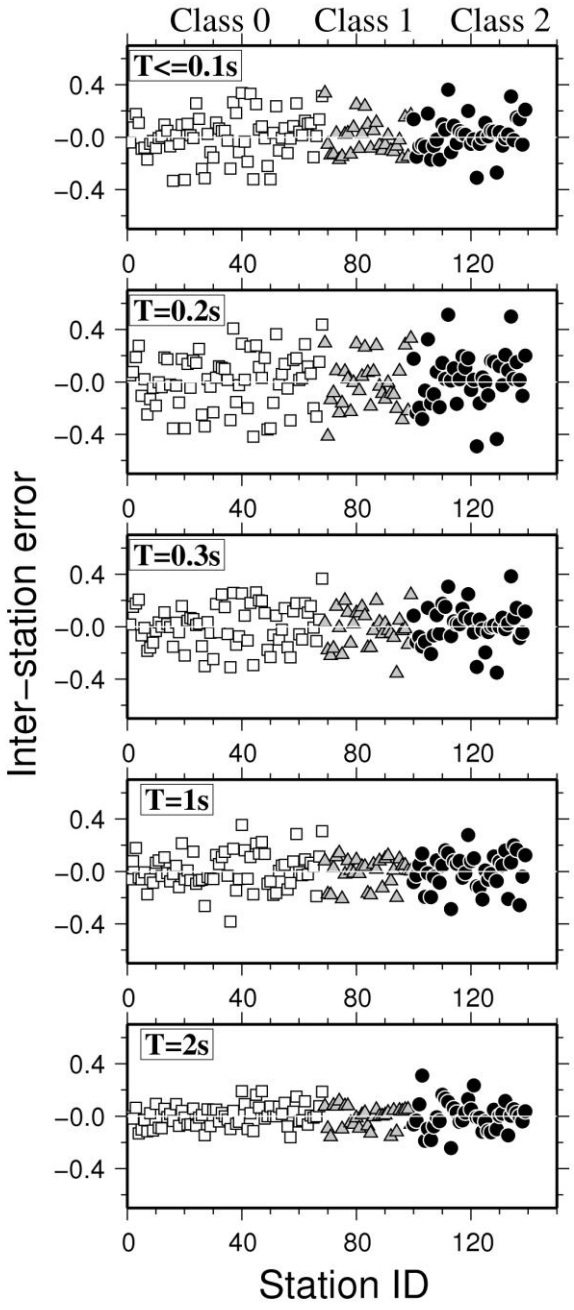
Class 0
Class 1
Class 2
T<=0.1s
T=0.2s
T=0.3s
T=1s
T=2s
0.4
−0.0
−0.4
0
40
80
120
Inter−station error
Station ID

Figure 9

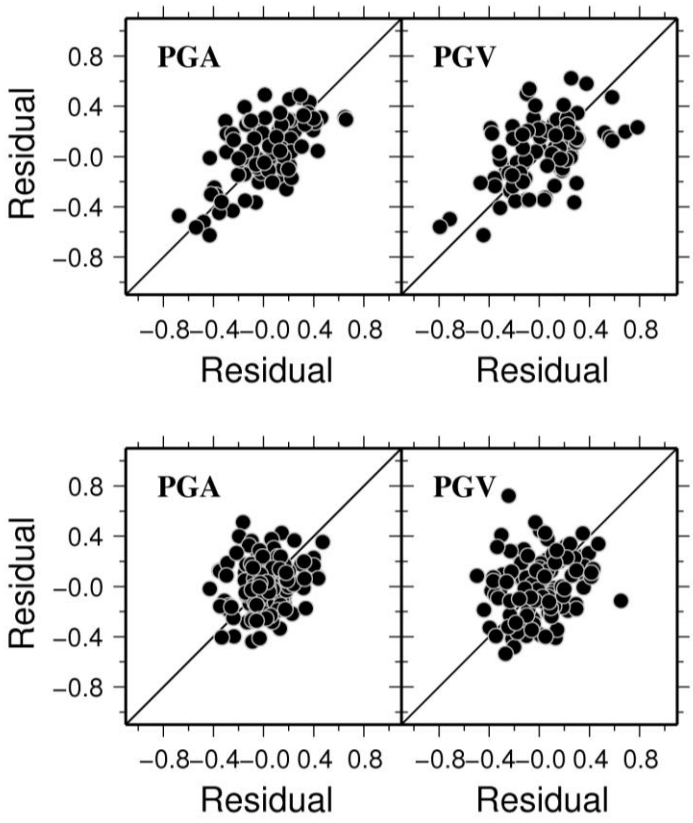
PGA
PGV
Residual
Residual
Residual
0.8
0.4
−0.0
−0.4
−0.8
−0.8 −0.4 −0.0 0.4 0.8

Figure 10

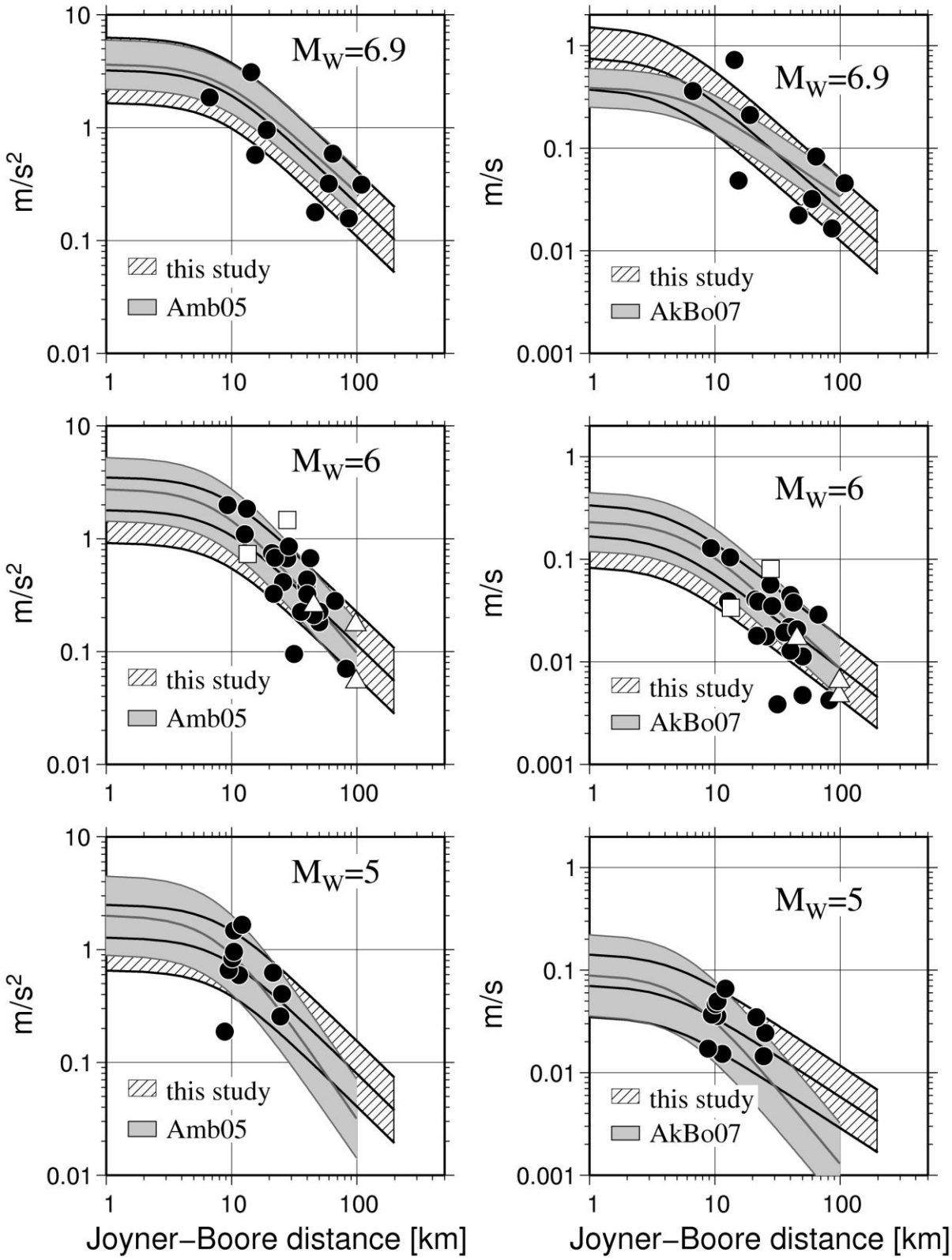
M_W=6.9
this study
Amb05
m/s²
M_W=6.9
this study
AkBo07
m/s
M_W=6
this study
Amb05
m/s²
M_W=6
this study
AkBo07
m/s
M_W=5
this study
Amb05
m/s²
M_W=5
this study
AkBo07
m/s
Joyner−Boore distance [km]
Joyner−Boore distance [km]

Figure 11

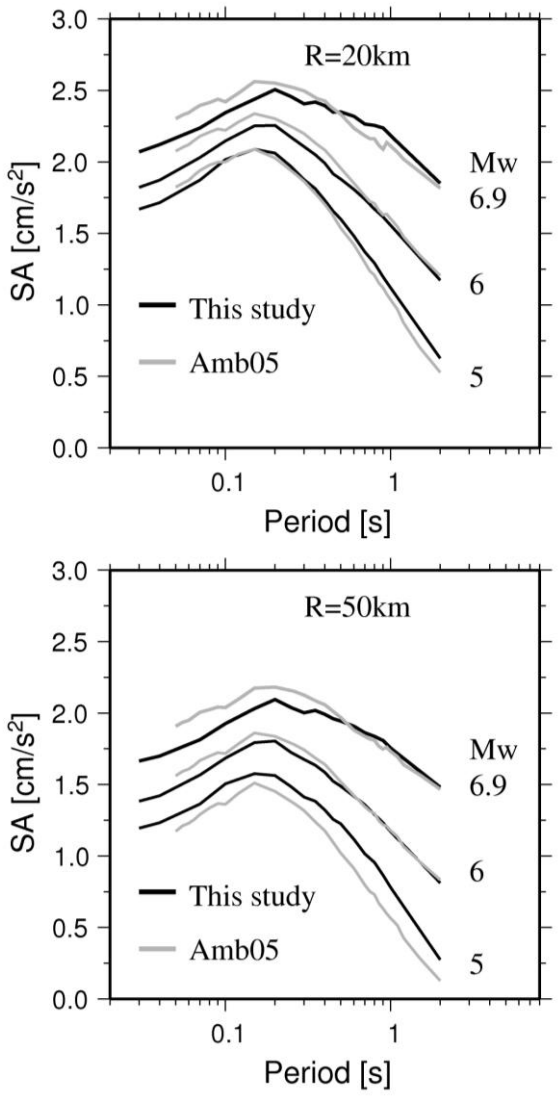
R=20km
SA [cm/s²]
Period [s]
Mw
6.9
6
5
This study
Amb05
R=50km
SA [cm/s²]
Period [s]
Mw
6.9
6
5
This study
Amb05

Figure 12

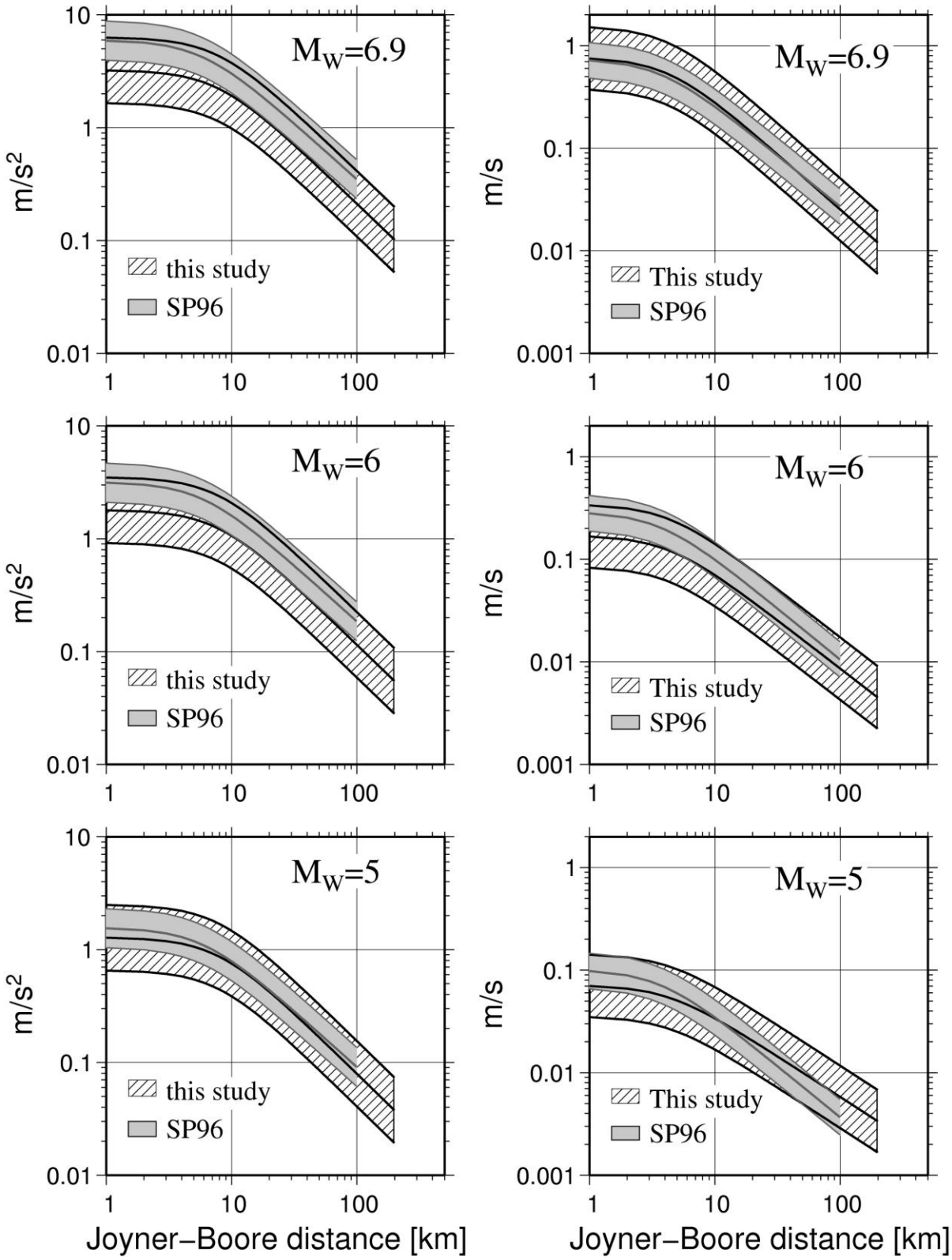
M_W=6.9
this study
SP96
m/s²
M_W=6.9
This study
SP96
m/s
M_W=6
this study
SP96
m/s²
M_W=6
This study
SP96
m/s
M_W=5
this study
SP96
m/s²
M_W=5
This study
SP96
m/s
Joyner−Boore distance [km]
Joyner−Boore distance [km]

Figure 13

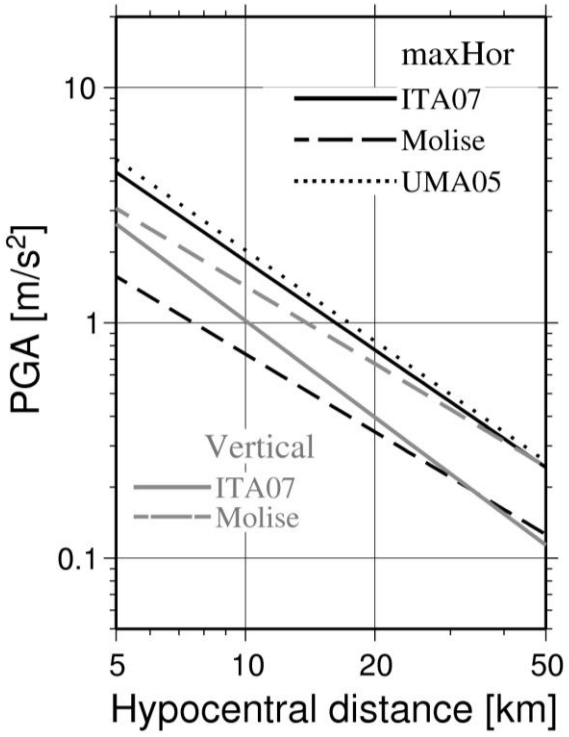
maxHor
ITA07
Molise
UMA05
Vertical
ITA07
Molise
PGA [m/s2]
10
1
0.1
5
10
20
50
Hypocentral distance [km]

Figure 14

Copyright Form

This piece of the submission is being sent via mail.